

# Initial state fluctuations from SPS to LHC

J. Milošević

University of Belgrade and  
Vinča Institute of Nuclear Sciences,  
Belgrade, Serbia

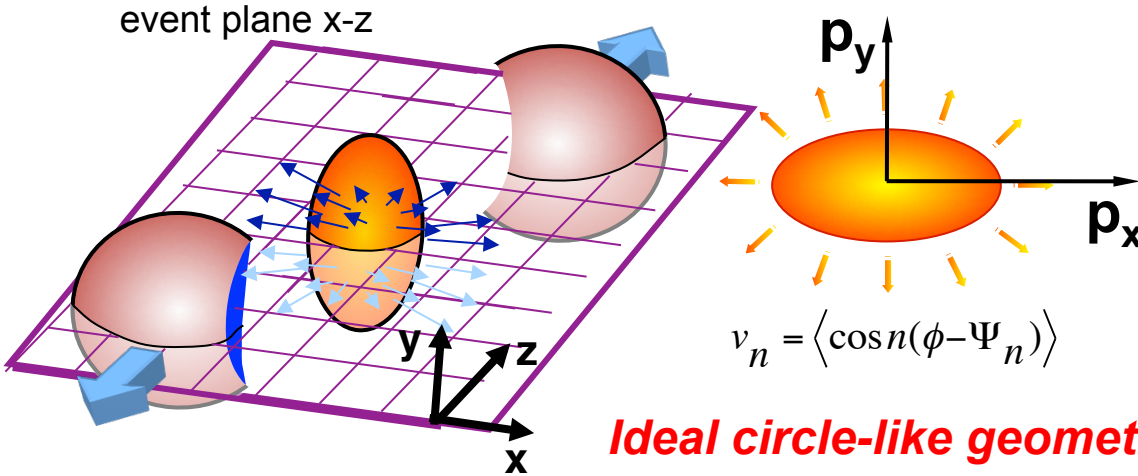


# Outline

- ❖ Azimuthal anisotropy
  - ✧ conventional methods
  - ✧ Initial-state fluctuations (ISF) and higher order Fourier harmonics
- ❖ Triangular flow at SPS, RHIC and LHC energies
- ❖ Collectivity over a wide  $p_T$  range in PbPb collisions
- ❖ Collectivity in small pPb and smallest pp collision systems
- ✧ ISF on sub-nucleonic level
- ❖ Factorization breaking – mechanism
  - $p_T$  dependent event plane
  - $\eta$  dependent event plane
- ❖ Principal Component Analysis (PCA) – method
- ❖ PCA method in flow physics – leading and sub-leading flow modes
- ❖ The PCA analysis in pPb and PbPb collisions at the LHC energy
- ❖ Conclusions

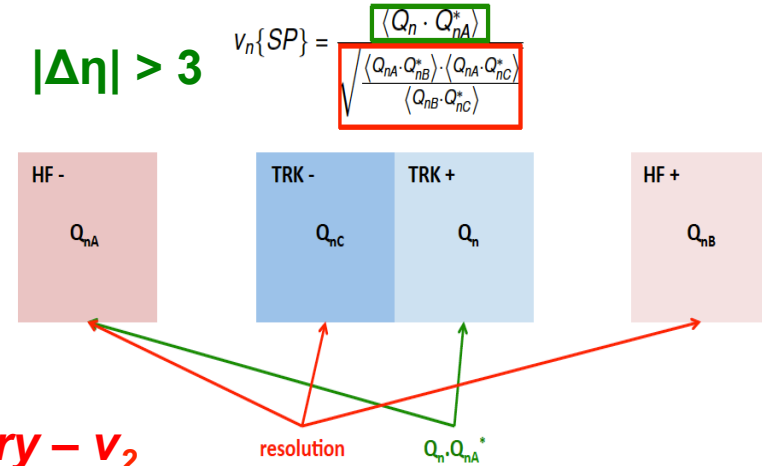
# Anisotropy harmonics $v_n$ – conventional methods

## Event Plane (EP) method



*Ideal circle-like geometry –  $v_2$*

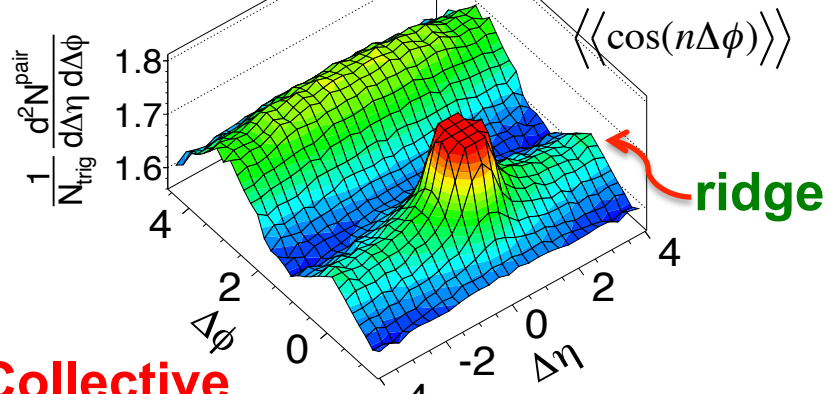
## Scalar Product (SP) method



## two-particle correlation method

pPb 5.02 TeV  
 $1 < p_T < 3$  GeV/c

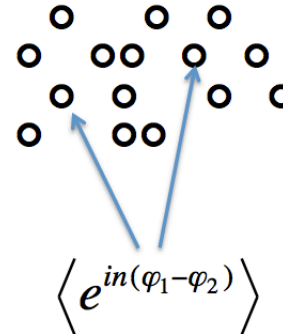
**0-3% centrality**  
 **$N > 110$**



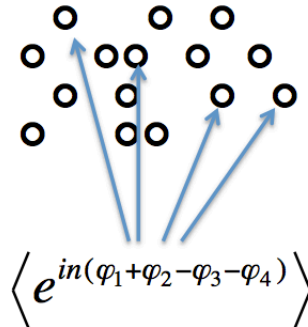
**Collective behavior?**

PLB 718 (2013) 795

## four-particle cumulant method



Advantage wrt 2-part.corr.:  
 removes two- and three-particle non-flow correlation



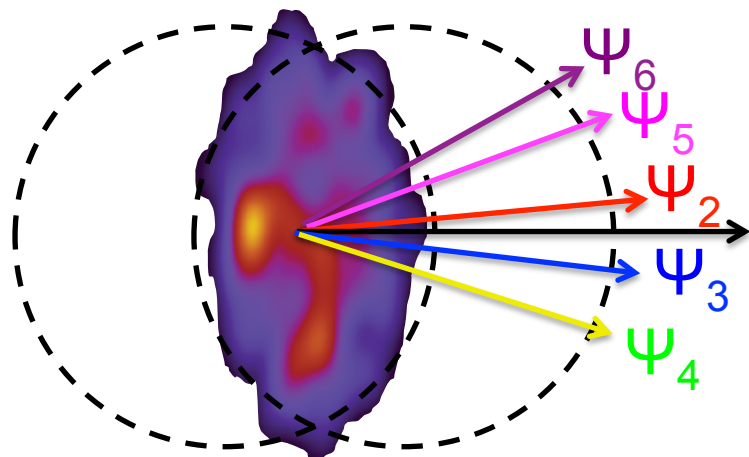
◆  $v_n$  from even higher order cumulants:  
 $v_n\{6\}, v_n\{8\}, \dots$

**Lee-Yang zero method**  
 correlates all particles of interest

# Role of initial state fluctuations (ISF) on anisotropy

## Anisotropy harmonics with order higher than 2

geometry –  $v_2$   
ISF –  $v_3$

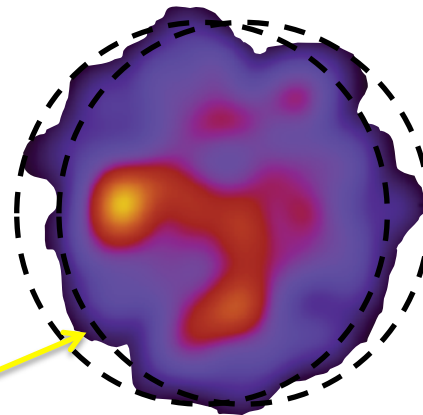


$v_2, v_3, v_4, v_5$  and  $v_6$   
using multiple methods

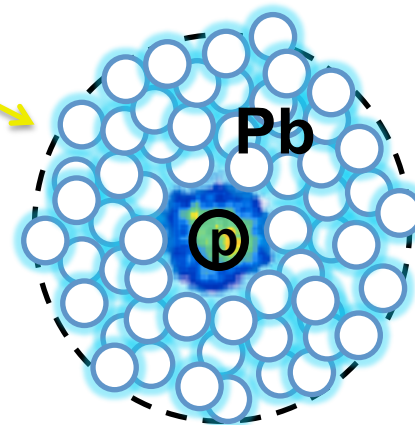
Simple, circle-like geometry does not describe the formed system precisely enough

initial-state fluctuations dominates

## Ultra-central collisions



## Asymmetric (pPb) high-multiplicity collisions



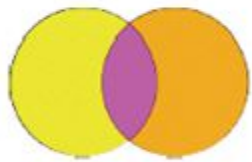
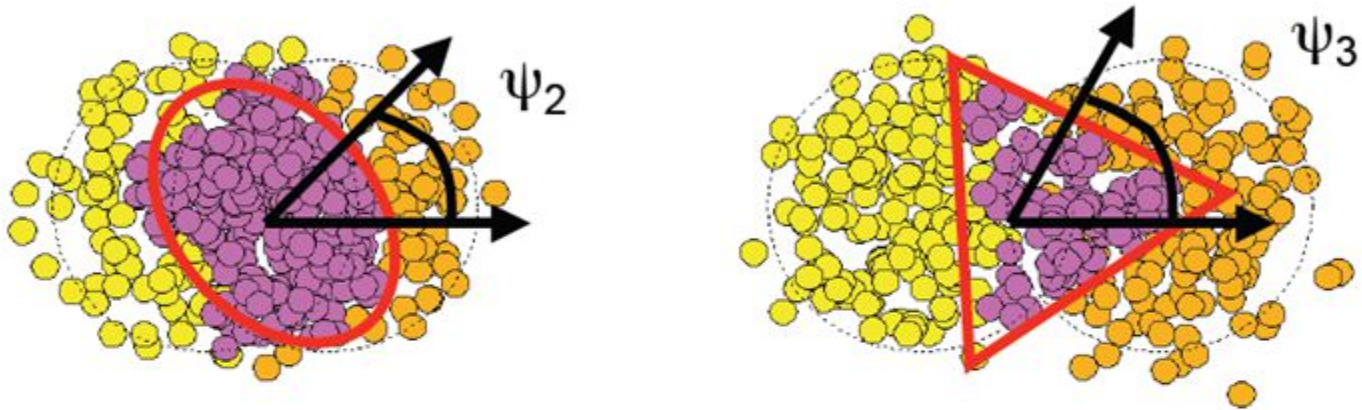
Phys.Rev. C89 (2014) 044906  
(arXiv:1310.8651)

JHEP 1402 (2014) 088  
(arXiv:1312.1845)

Phys.Lett. B724 (2013) 213  
(arXiv:1305.0609)



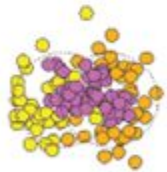
# Triangular flow – one of higher order Fourier harmonics



$$\frac{dN}{d\phi} = \frac{N}{2\pi} \left( 1 + \sum 2v_n \cos(n(\phi - \psi_R)) \right)$$

$$v_2 = \langle \cos(2(\phi - \psi_R)) \rangle$$

$$v_3 = 0$$



$$\frac{dN}{d\phi} = \frac{N}{2\pi} \left( 1 + \sum 2v_n \cos(n(\phi - \psi_n)) \right)$$

$$v_2 = \langle \cos(2(\phi - \psi_2)) \rangle$$

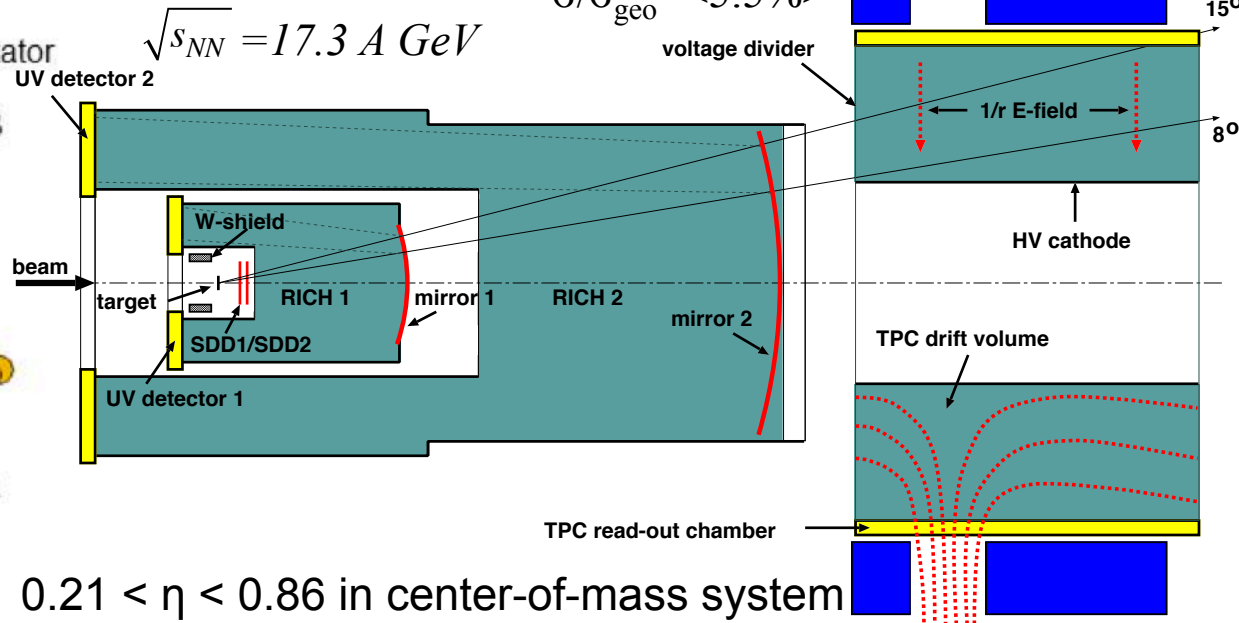
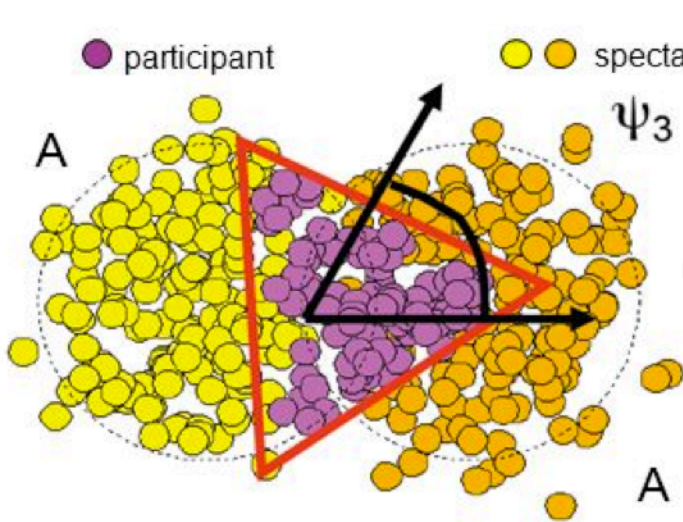
$$v_3 = \langle \cos(3(\phi - \psi_3)) \rangle$$

The triangular initial shape → triangular hydrodynamic flow

**B. Alver and G. Roland**  
**PRC 81(2010) 054905**

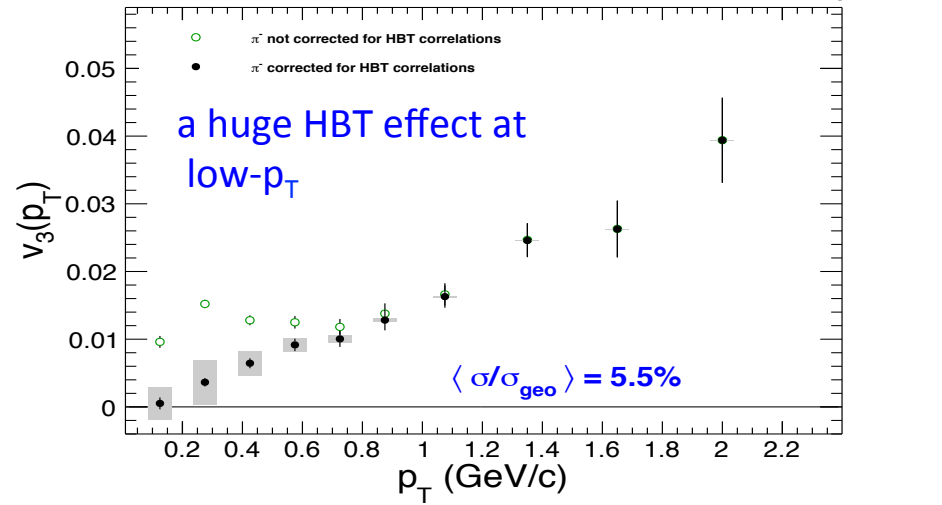
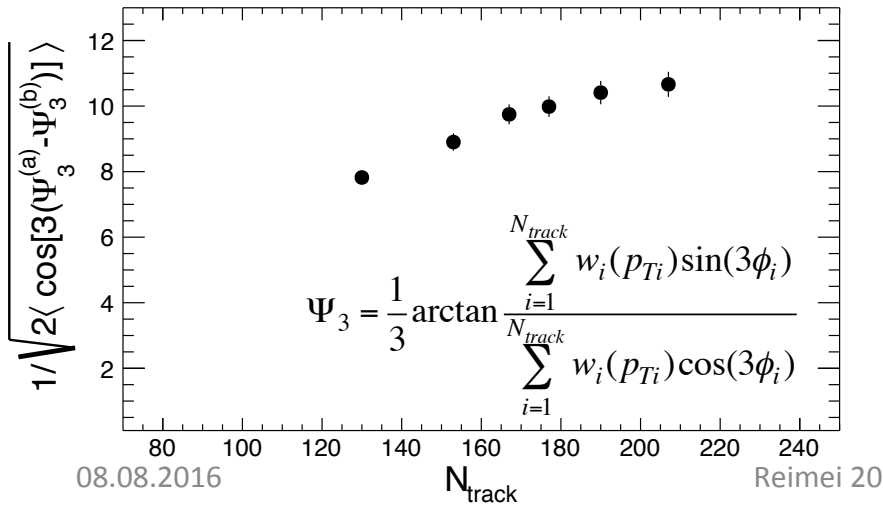
# Triangular flow in PbAu at the top SPS energy

≈30M PbAu collisions collected during 2000 data taking period



EP method is used

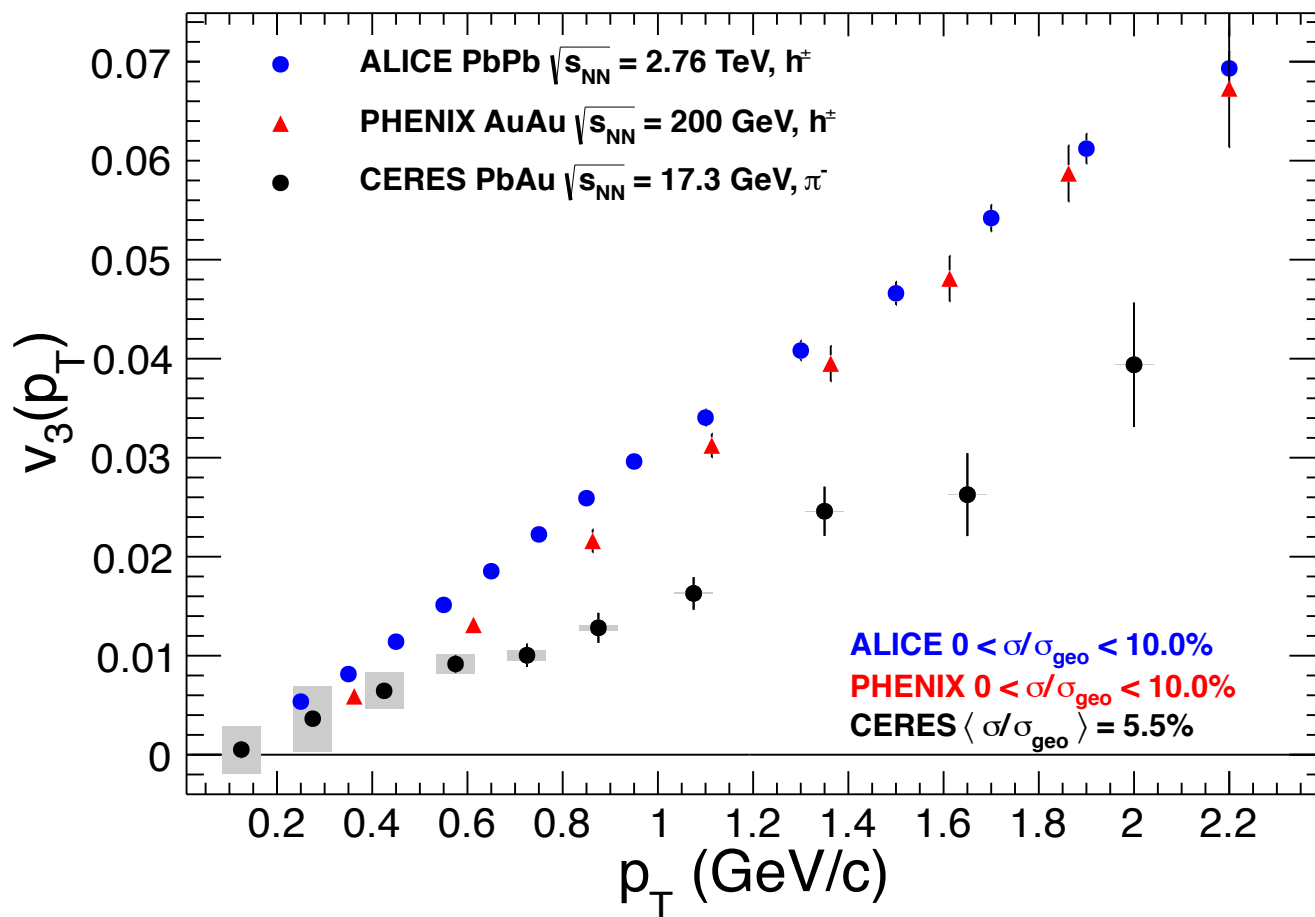
accepted to Nucl.Phys.A



# $v_3$ vs $p_T$ – comparison to other experiments

- ❖ First  $p_T$  dependent measurement of the triangular flow at the top SPS energy
- ❖ Top RHIC and LHC energy gives very similar  $v_3$  magnitudes
- ❖ The  $v_3$  at the top SPS energy is about half of those at top RHIC and LHC
- ❖ Linear increase but with different slopes

accepted to Nucl.Phys.A



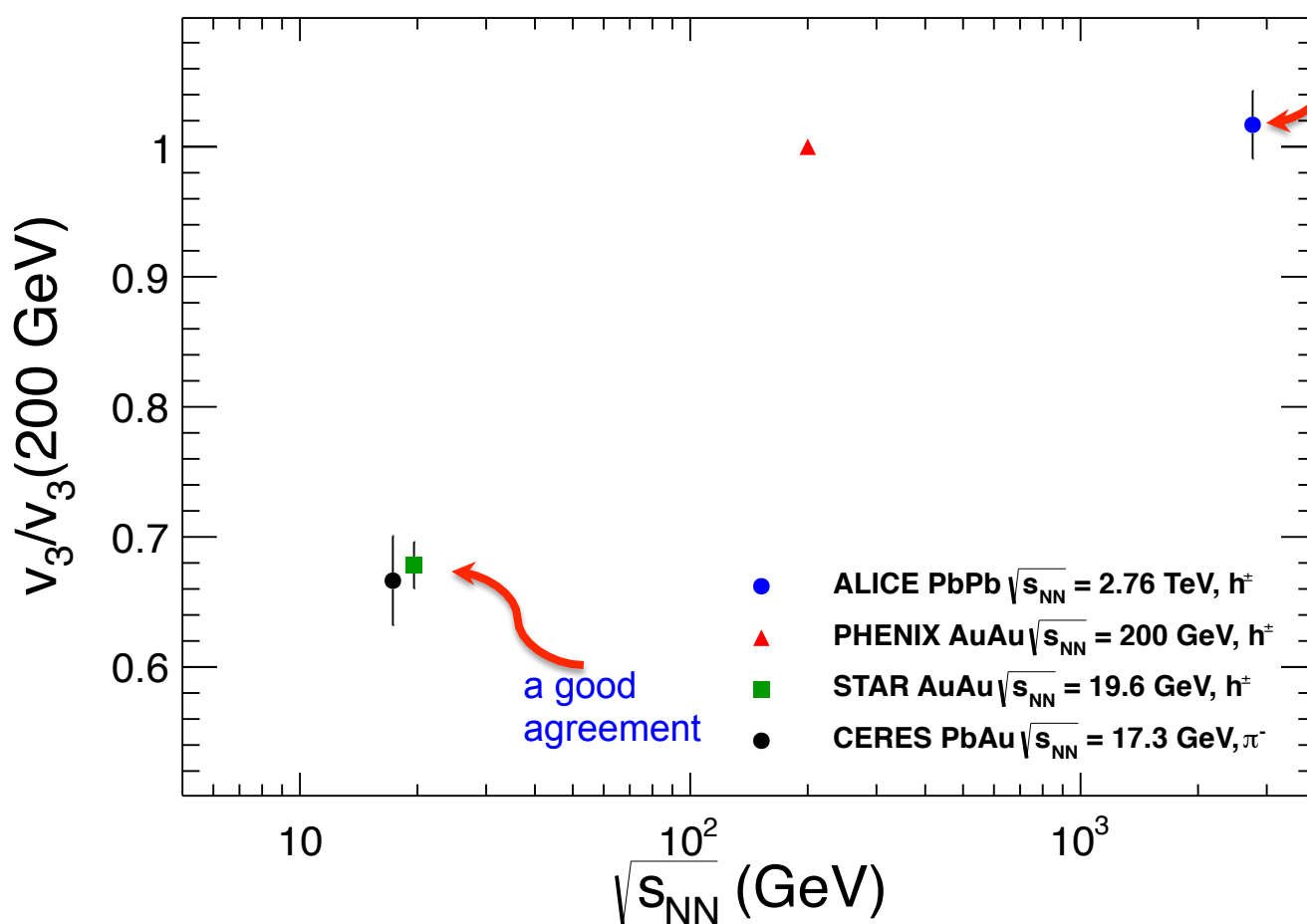
- ◇ Note limited  $p_T$  range restricted to the CERES acceptance
- ◇ ALICE uses large  $|\Delta\eta|$  gaps
- ◇ Jet yield is for more than one order of magnitude smaller at SPS
- ◇ No option to include  $|\Delta\eta|$  gap at CERES

PHENIX  
**PRL 107 (2011) 252301**  
 ALICE  
**PLB 719 (2013) 18**

# Energy dependence

- ❖ RHIC 19.6 GeV is quite close to the top SPS energy of 17.3 GeV
- ❖ Comparison is done at very similar centralities ( $\langle \sigma / \sigma_{\text{geo}} \rangle \approx 5\%$ )
- ❖ A rather good agreement with an AMPT prediction for the ratio of about 0.6 at 19.6 GeV RHIC energy

Accepted to Nucl.Phys.A



same  $v_3$  at the top RHIC and LHC

✧ As a referent level is taken  $v_3$  value at the top RHIC energy

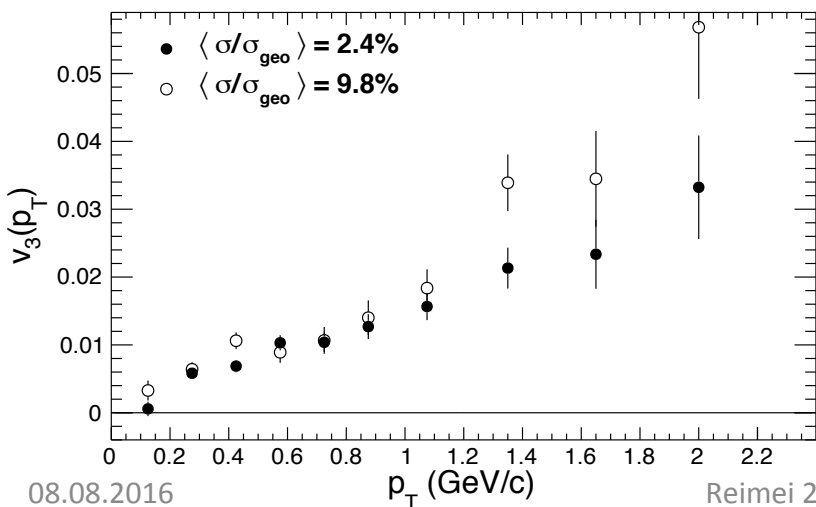
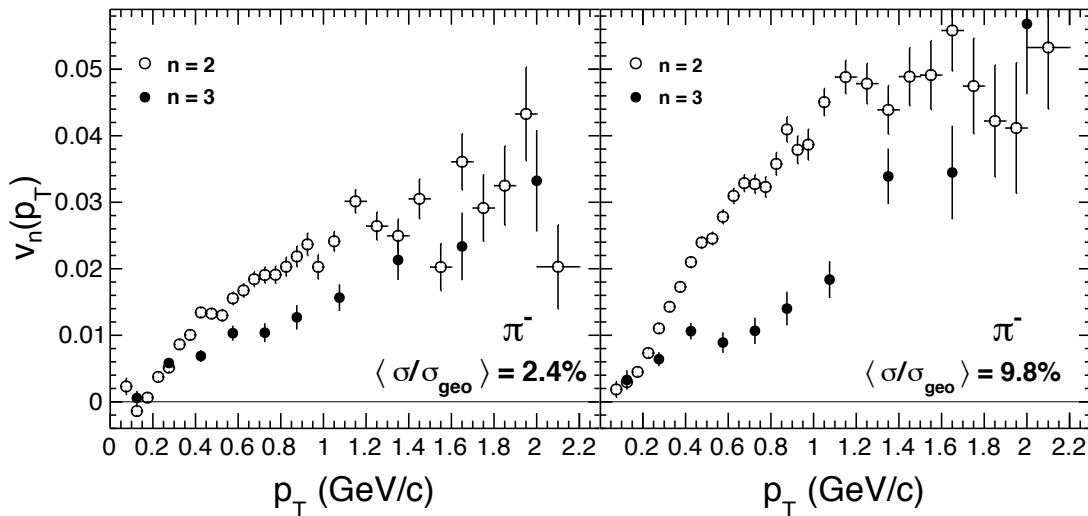
✧  $v_3$  values integrated over  $0.3 < p_T < 2.1 \text{ GeV}/c$  !

PHENIX  
**PRL 107 (2011) 252301**  
 ALICE  
**PLB 719 (2013) 18**  
 STAR  
**PRL 116 (2016) 112302**

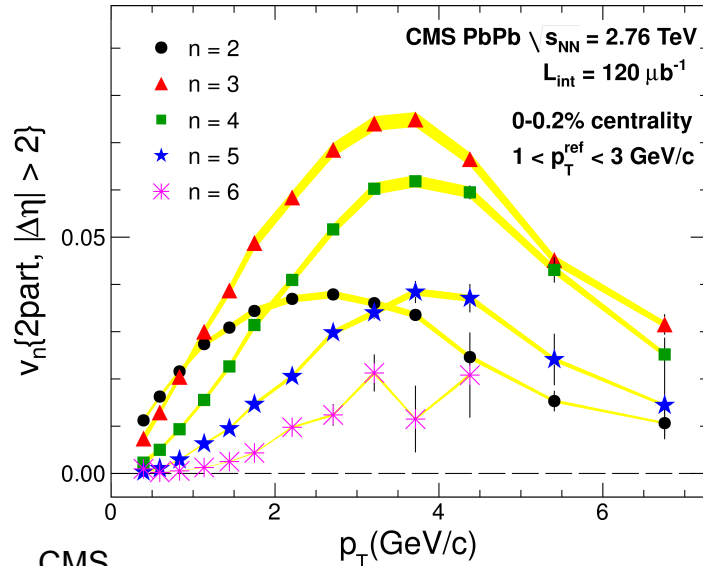
# $v_3$ in comparison with $v_2$

- ❖ **Elliptic flow** reflects the initial anisotropy and thus **depends strongly on centrality**
- ❖ **Triangular flow** comes from the ISF and **weakly depends on centrality**
- ❖ The different centrality behavior between  $v_2$  and  $v_3$
- ❖ For very central collisions ( $\langle \sigma/\sigma_{\text{geo}} \rangle = 2.4\%$ ),  $v_3$  becomes close to the  $v_2$

accepted to Nucl.Phys.A



✧ Triangular flow is dominant anisotropy for ultra-central collisions at the LHC energies

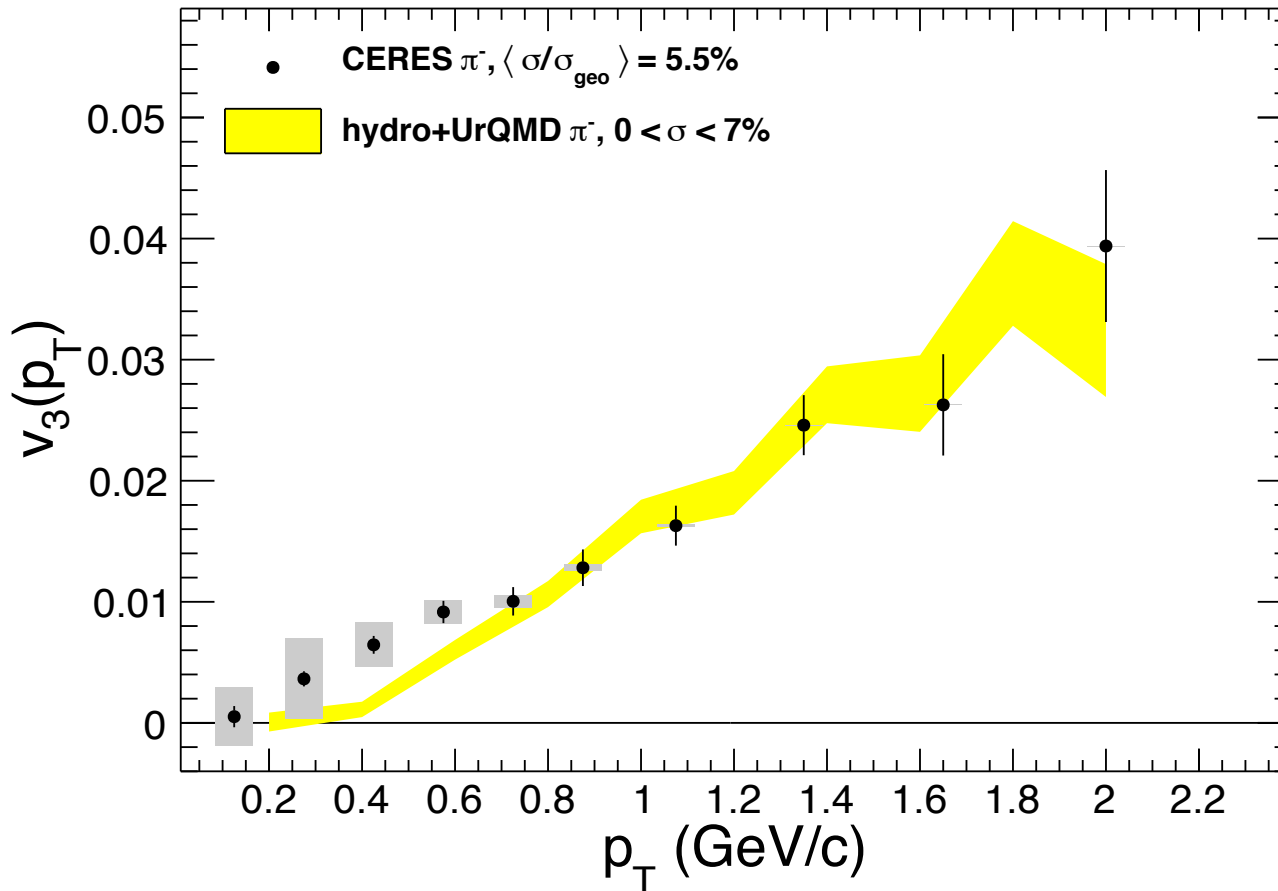


CMS  
JHEP 1402 (2014) 088

# Comparison with hydro+UrQMD predictions

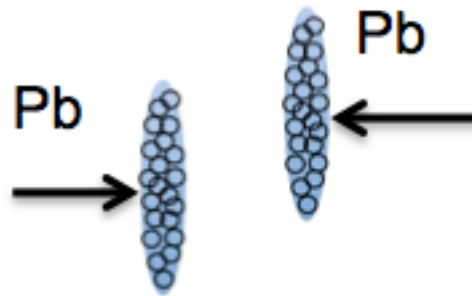
- ❖ Relativistic hydrodynamics + transport models (hybrid models)
- ✧ vHLLE viscous hydrosolver + UrQMD hadron cascade (I. Karpenko, P. Huovinen, H. Petersen and M. Bleicher **PRC 91 (2015) 064901**)
- ❖ The model predictions for hadrons within  $0.2 < p_T < 2.0$  GeV/c and  $-1 < \eta < 1$
- ❖ Centrality samples roughly correspond to the experimental ones

accepted to Nucl.Phys.A

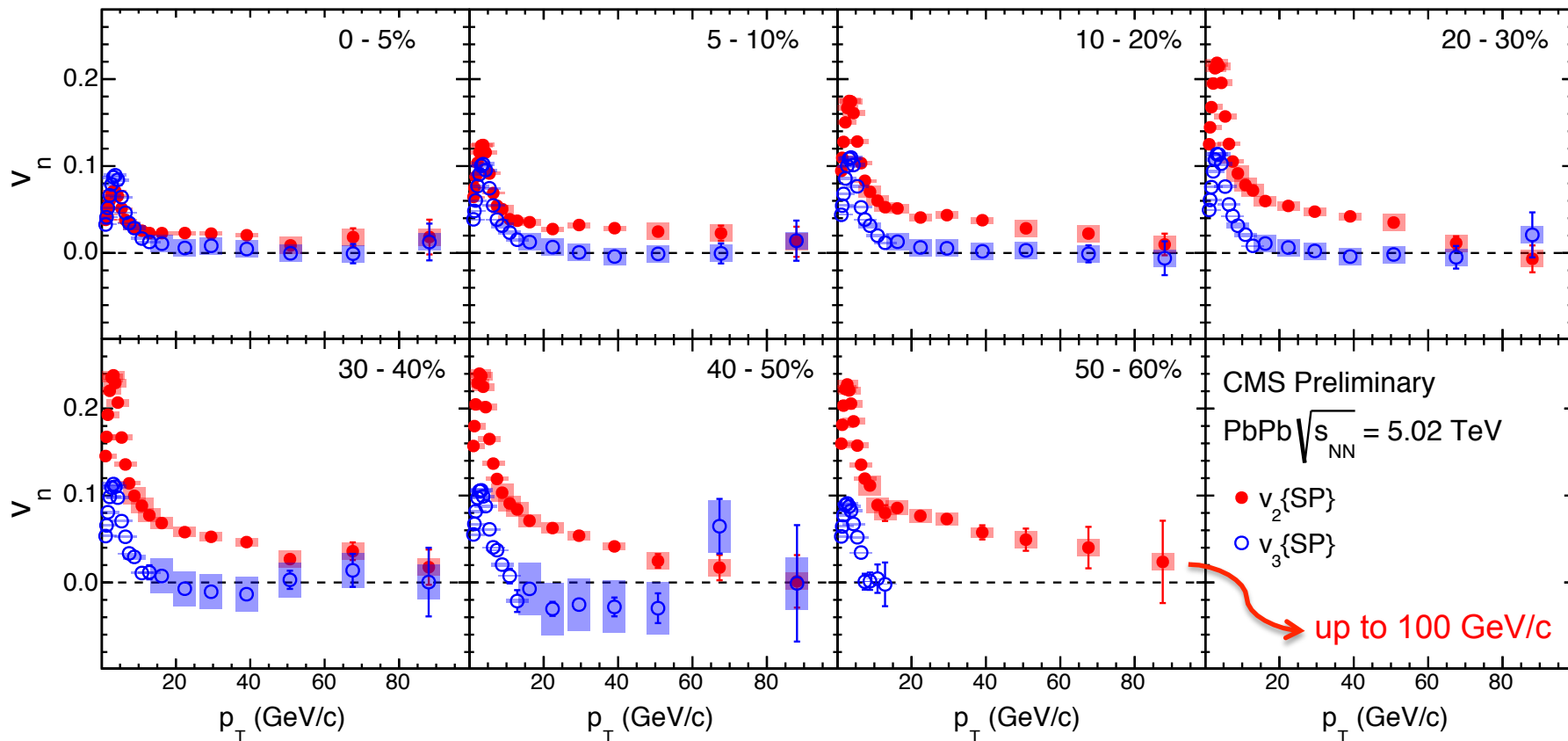


- ✧ Particization at constant energy density  $0.5 \text{ GeV fm}^3$
- ✧ Kinetic and chemical freeze-out are dynamical
- ✧ Model predictions in a very good agreement with the CERES results
- ✧ A small disagreement appears at low- $p_T$

# Collectivity over a wide $p_T$ range in PbPb



# $v_n\{\text{SP}\}$ over a wide $p_T$ range

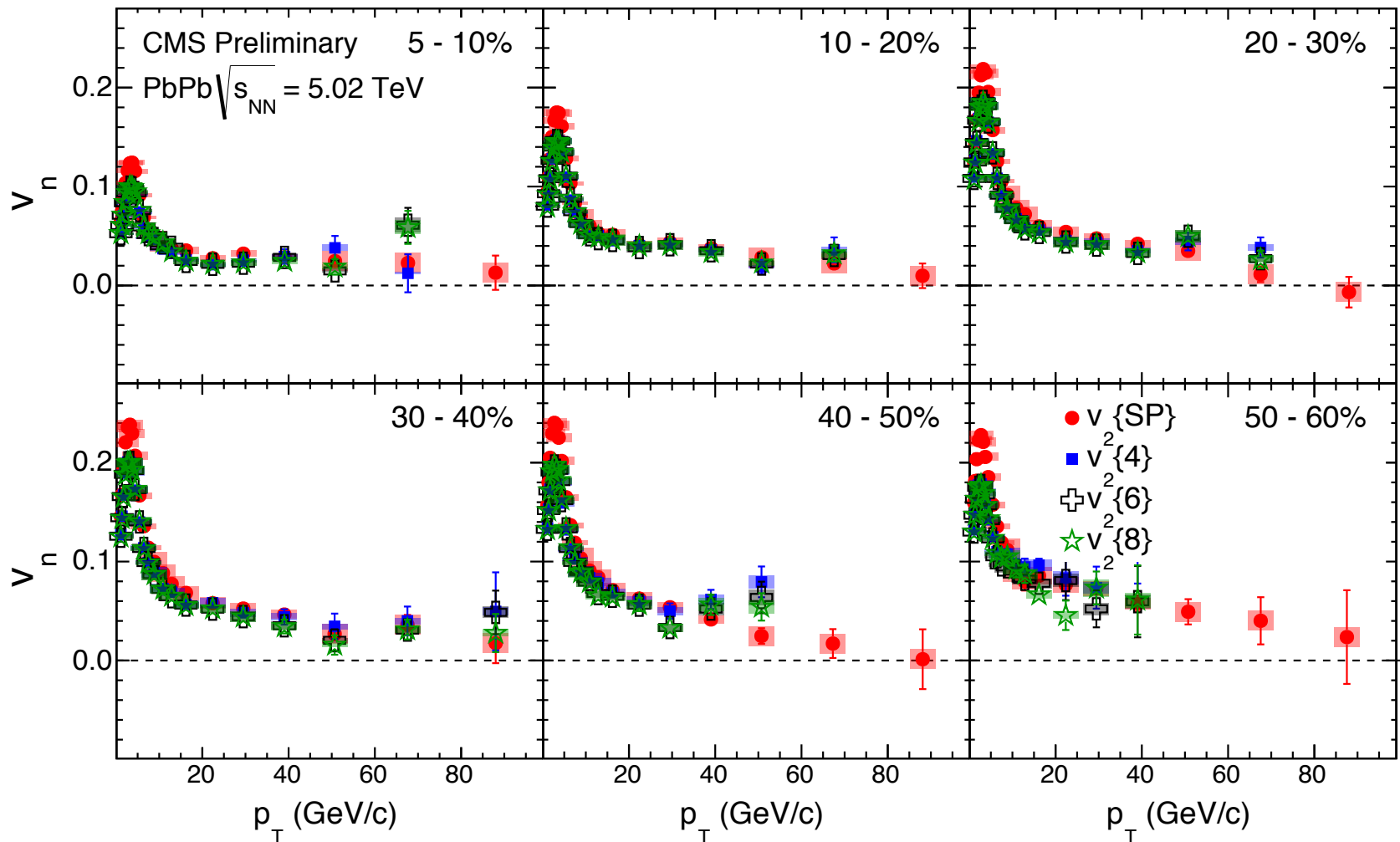


CMS PAS HIN-15-014

- ❖ low- $p_T$  - hydrodynamic flow ( $v_2$  – geometry,  $v_3$  – ISF on nucleonic level)
- ❖  $v_2$  non-zero up to very high  $p_T$
- ❖ high- $p_T$  - may reflect the path-length dependence of parton energy loss
- ❖  $v_2$  is complementary to  $R_{\text{AA}}$  measurements
- ❖  $v_3$  mainly consistent with zero at high- $p_T$



# Collectivity over a wide $p_T$ range

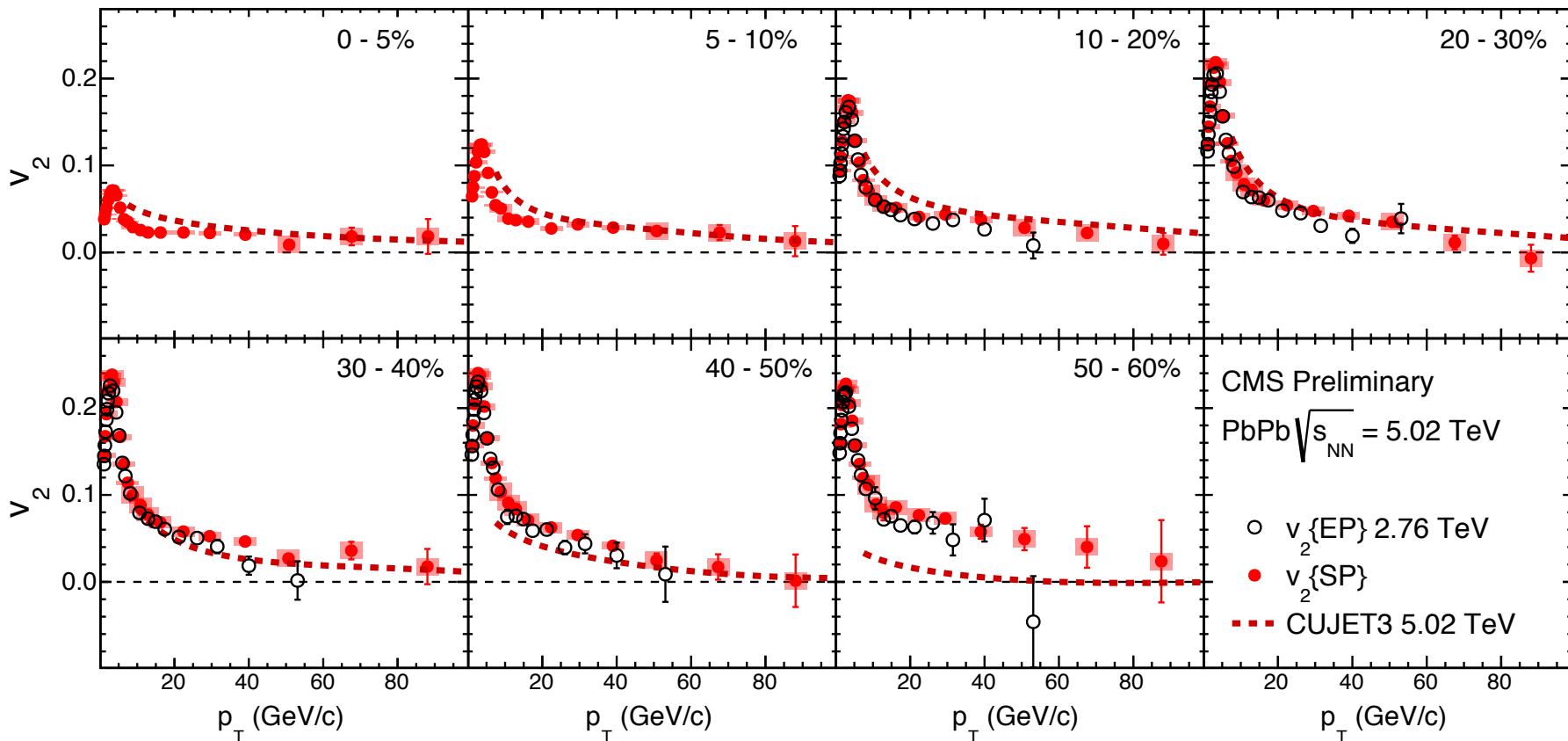


CMS PAS HIN-15-014

- ❖ low- $p_T$  – ratio  $v_2\{2k\}/v_2\{SP\} \approx 0.8$  and  $v_2\{4\} \approx v_2\{6\} \approx v_2\{8\}$  ← hydrodynamics
- ❖ high- $p_T$  – SP and multi-particle correlation tend to converge to the same value
- ❖  $v_2\{4\} \approx v_2\{6\} \approx v_2\{8\} \neq 0$  ← collectivity (likely to be related to jet quenching)

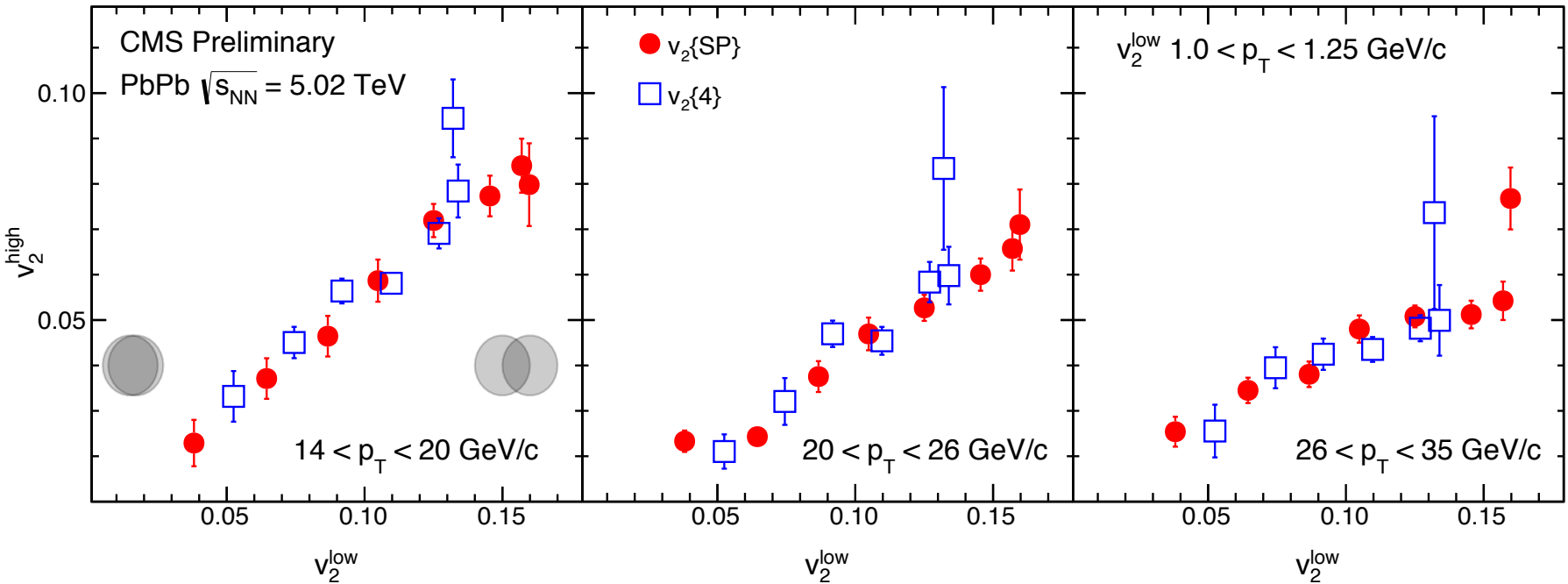
# Comparison with lower energy and CUJET3

CMS PAS HIN-15-014



- ❖ A slight increase of  $v_2$  wrt results (EP method) from 2.76 TeV collision energy
- ❖ CUJET3 predictions roughly compatible with the data at high- $p_T$  (over 40 GeV/c)
- ❖ At lower  $p_T$ , CUJET3 overpredicts the experimental  $v_2$

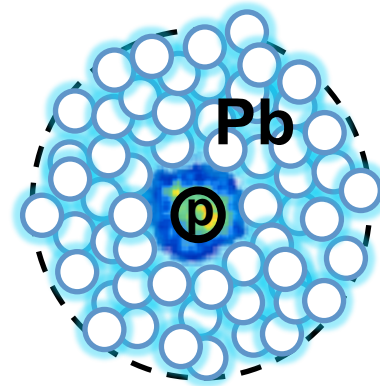
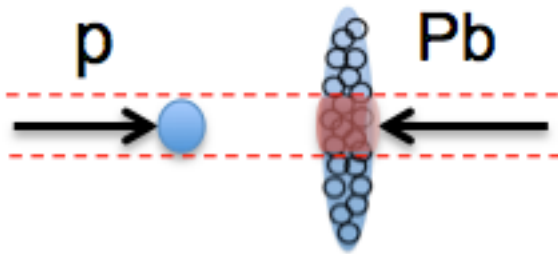
# Collectivity over a wide $p_T$ and centrality range



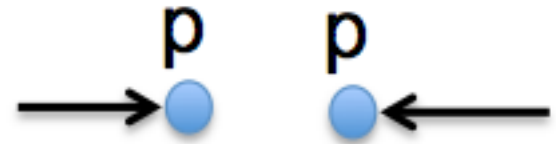
CMS PAS HIN-15-014

## Soft and hard correlation

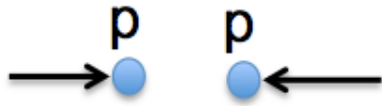
- ❖ Correlation between low- $p_T$   $v_2$  and high- $p_T$   $v_2$  over a wide centrality range
- ❖ Each point represents one centrality bin
- ❖ Strong correlation may indicate that low- $p_T$   $v_2$  and high- $p_T$   $v_2$  may have the same origin
- ❖ Within uncertainties, slopes between  $v_2\{SP\}$  and  $v_2\{2k\}$  are compatible
- ❖ Extrapolations compatible to 0 within uncertainties



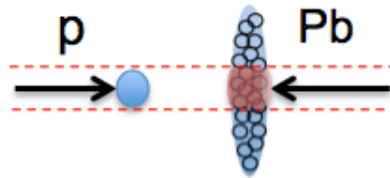
## Collectivity in small pPb and smallest pp systems?



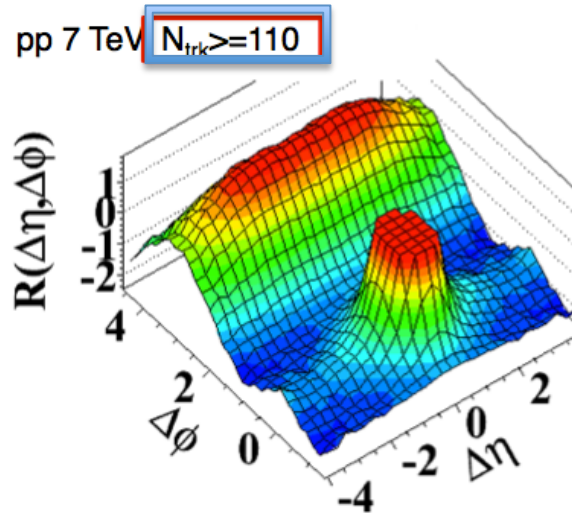
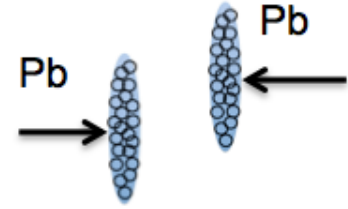
# The ridge seen in all colliding systems at LHC



high-multiplicity



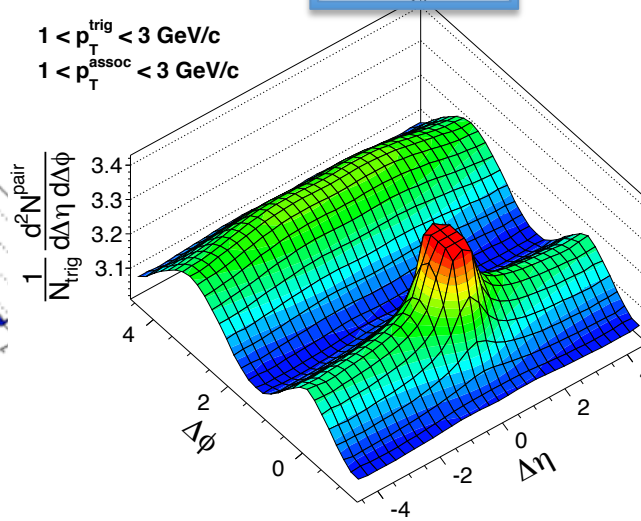
high-multiplicity



JHEP 09 (2010) 091

CMS pPb  $\sqrt{s_{NN}} = 5.02$  TeV,  $220 \leq N < 260$

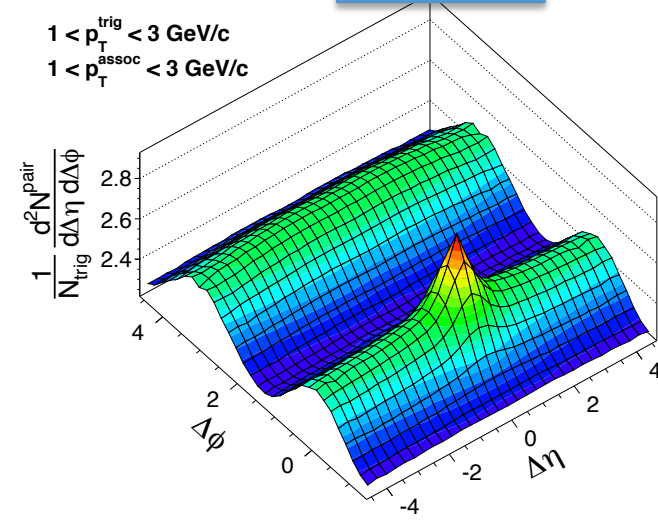
$1 < p_T^{trig} < 3$  GeV/c  
 $1 < p_T^{assoc} < 3$  GeV/c



PLB 718 (2013) 795

CMS PbPb  $\sqrt{s_{NN}} = 2.76$  TeV,  $220 \leq N < 260$

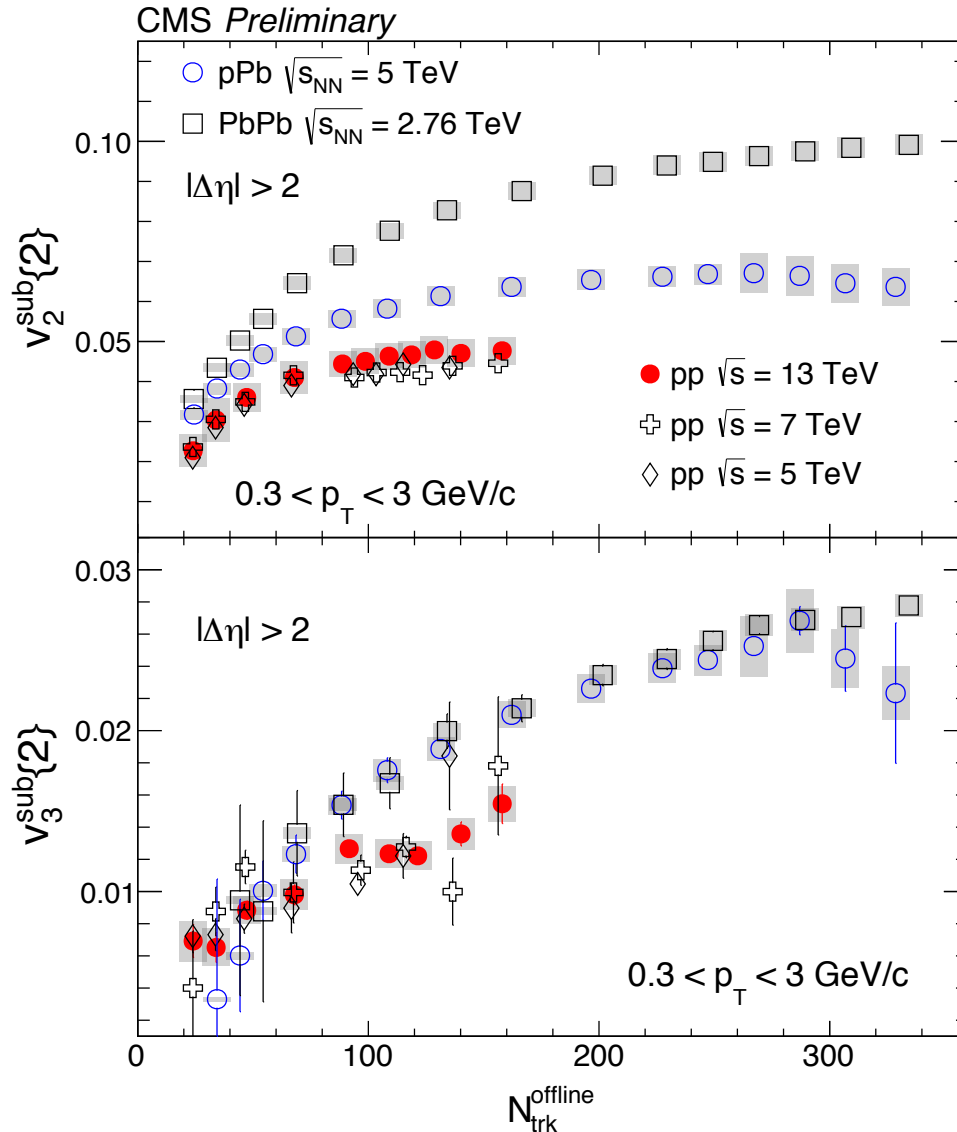
$1 < p_T^{trig} < 3$  GeV/c  
 $1 < p_T^{assoc} < 3$  GeV/c



PLB 724 (2013) 213

- ❖ Does the ridge in  $pp$  and  $pPb$  collisions originate from hydrodynamics flow like in  $PbPb$  collisions or it is connected with color-glass condensate (CGC)

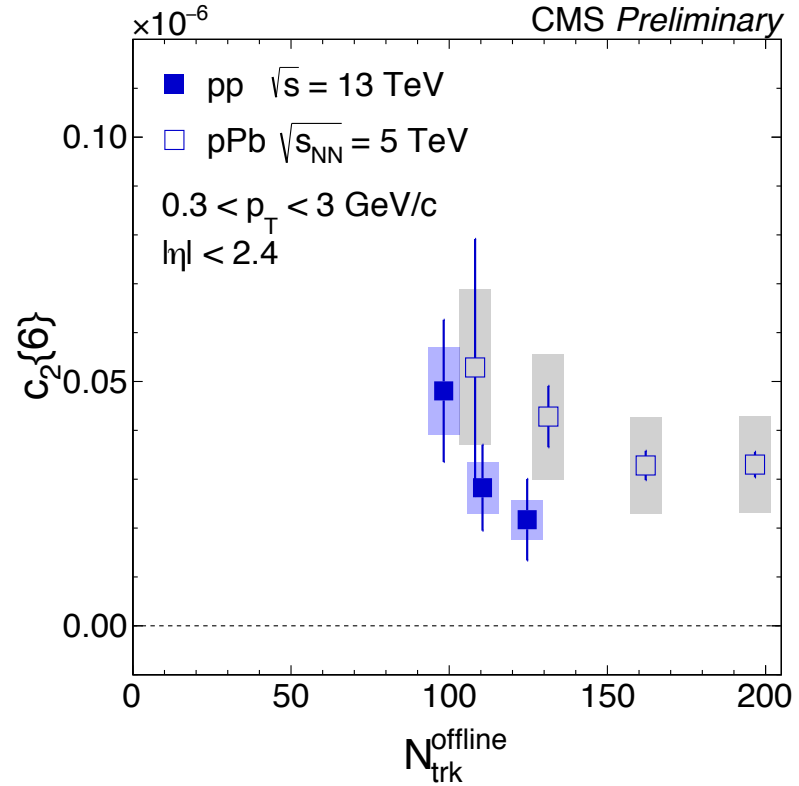
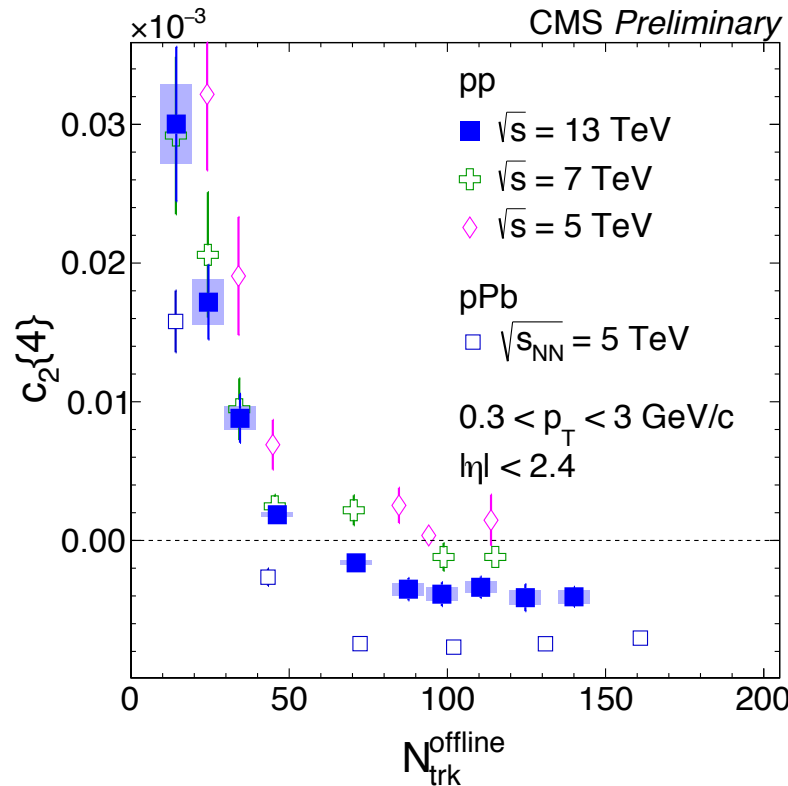
# $v_2\{2\}$ and $v_3\{2\}$ in pp at different collision energies



- ❖ There is no or a very weak energy dependence of  $v_2$  in pp collisions
- ❖  $v_2\{2\}$  in pp collisions shows a similar pattern as the one seen in pPb collisions (gets flat at the highest multiplicities)
- ❖ The  $v_2\{2\}$  magnitude is ordered: it is highest in PbPb, gets smaller in pPb and become smallest in pp collisions
- ❖ In difference of the  $v_2$ , the  $v_3$  magnitude is comparable to those in pPb and PbPb collisions
- ❖ At low multiplicities, the systematic uncertainties are large for all the three systems
- ❖ At high multiplicities,  $v_3$  in pp increases at a slower rate than in pPb and PbPb systems

CMS PAS HIN-16-010

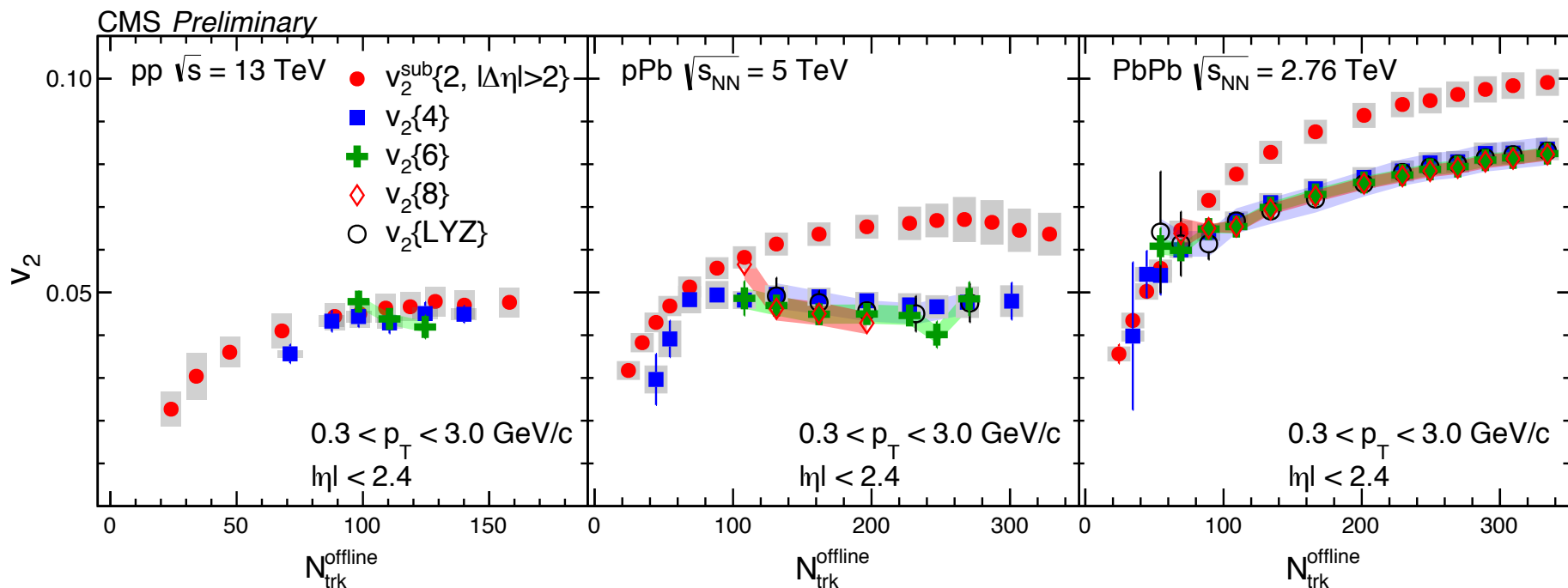
# $c_2\{4\}$ and $c_2\{6\}$ in pp at different collision energies



CMS PAS HIN-16-010

- ❖ Multi-particle correlations are used to reduce jet correlations from the away side and to explore collective nature of the long-range correlations in pp.
- ❖  $v_2\{4\}$  and  $v_2\{6\}$  are extracted
- ❖ Clear negative  $c_2\{4\}$  at high multiplicities in pp at 13 TeV is seen  $v_n\{4\} = \sqrt[4]{-c_n\{4\}}$
- ❖ and positive  $c_2\{6\}$   $v_n\{6\} = \sqrt[6]{\frac{1}{4}c_n\{6\}}$
- ❖ Statistical limitations

# $v_2$ in pp compared to pPb and PbPb results



$v_2\{2\} \geq v_2\{4\} \approx v_2\{6\}$   
 collectivity!

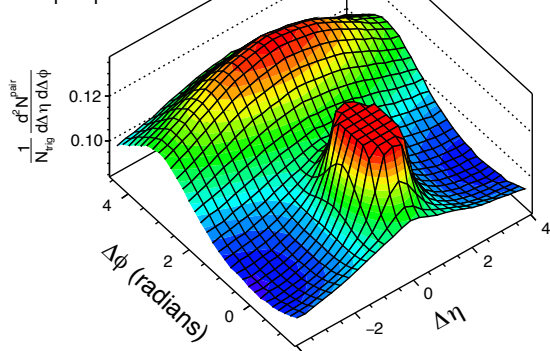
CMS PAS HIN-16-010

- ❖ Elliptic flow in pp measured using 2- and multi-particle correlations – compared to pPb and PbPb results
- ❖  $v_2\{2\}/v_2\{4\}(\text{pp}) \leq v_2\{2\}/v_2\{4\}(\text{pPb}) \leftarrow$  related to initial-state (IS) fluctuations
- ❖ smaller  $v_2\{2\}/v_2\{4\} \leftarrow$  less IS fluctuating sources (PRL 112 (2014) 082301)



CMS pp  $\sqrt{s} = 13$  TeV Preliminary

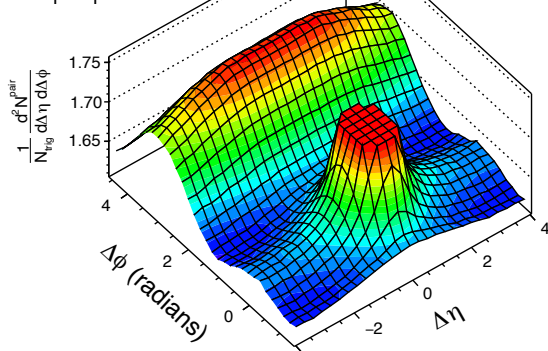
$10 \leq N_{\text{trk}}^{\text{offline}} < 20$   
 $1 < p_{\text{T}}^{\text{trig}}, p_{\text{T}}^{\text{assoc}} < 3$  GeV/c



$h^\pm - h^\pm$

CMS pp  $\sqrt{s} = 13$  TeV Preliminary

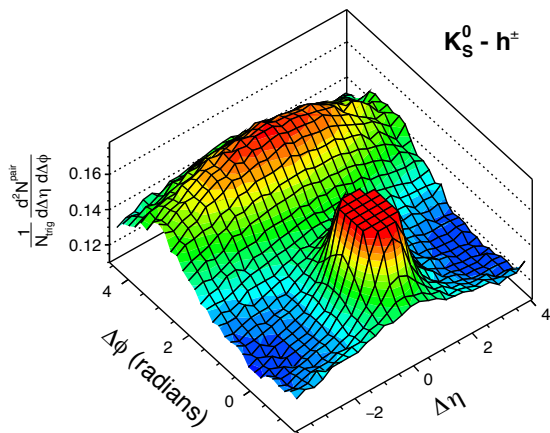
$105 \leq N_{\text{trk}}^{\text{offline}} < 150$   
 $1 < p_{\text{T}}^{\text{trig}}, p_{\text{T}}^{\text{assoc}} < 3$  GeV/c



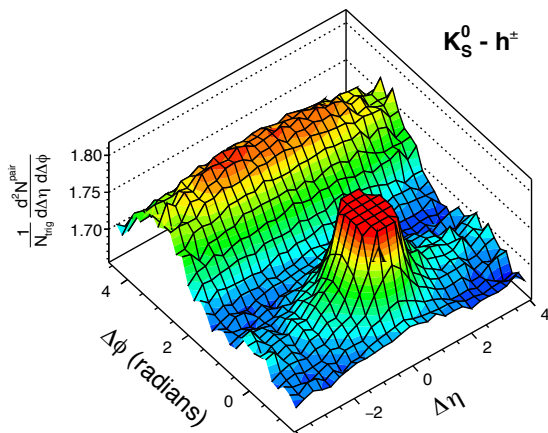
$h^\pm - h^\pm$

# 2D 2-particle corr. function in low- and high-multiplicity pp

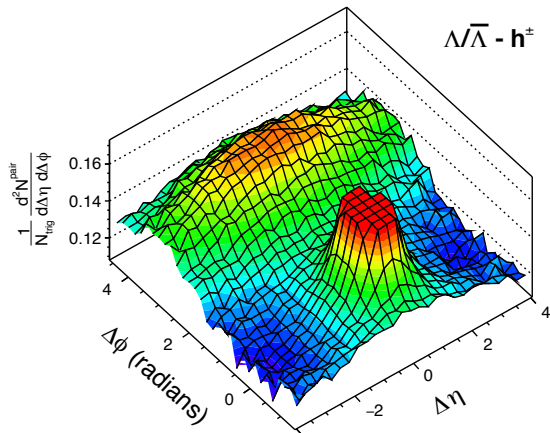
CMS PAS HIN-16-010



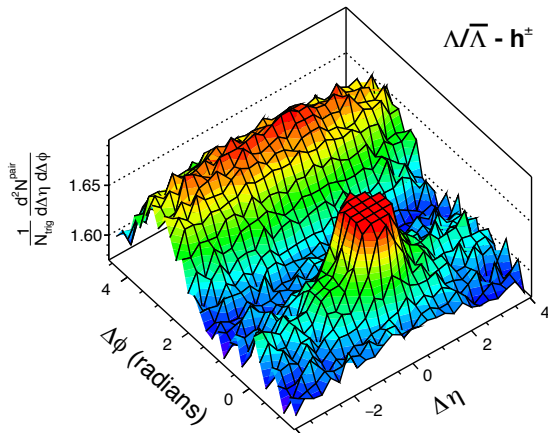
$K_S^0 - h^\pm$



$K_S^0 - h^\pm$



$\Lambda/\bar{\Lambda} - h^\pm$

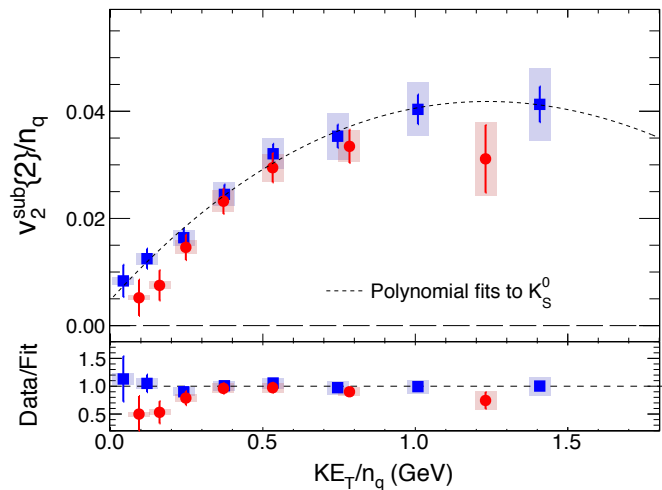
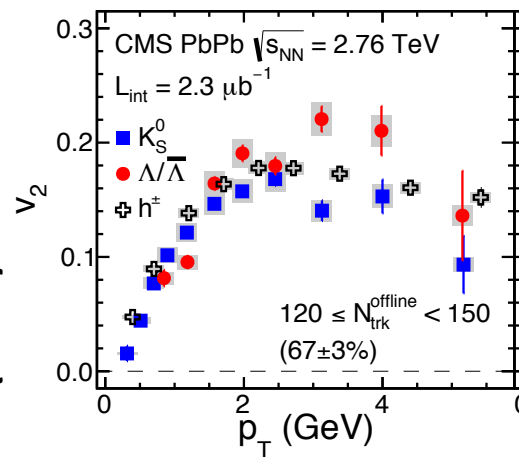
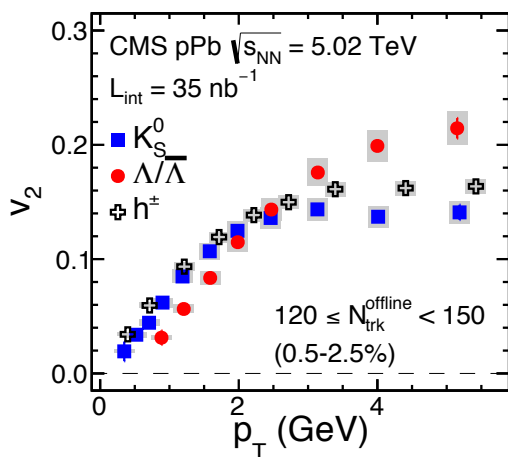
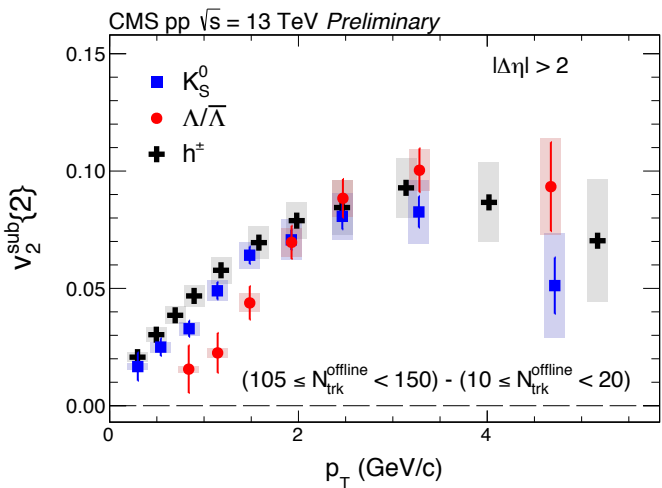


$\Lambda/\bar{\Lambda} - h^\pm$

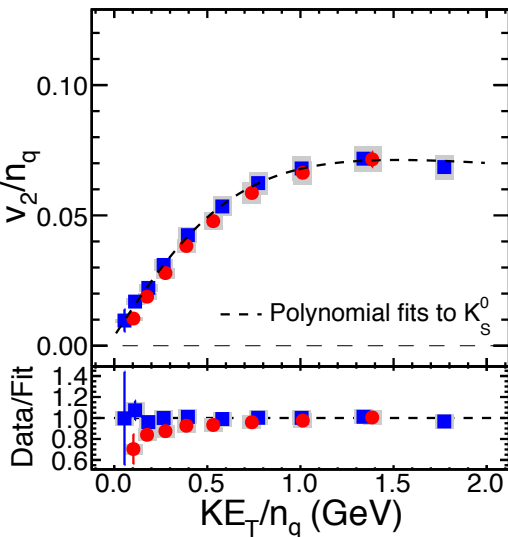
- ❖ charged-charged or charged-strange ( $K_S^0$  and  $\Lambda/\bar{\Lambda}$ ) particles
- ❖ particles are correlated within given multiplicity bin
- ❖ The ridge, at  $\Delta\phi \approx 0$  and elongated at  $\Delta\eta$ , is seen only in high-multiplicity pp events
- ❖ The ridge is present not only for charged, but also for strange particles
- ❖ What is the origin of the ridge in the smallest pp system?

collective behavior in pp?

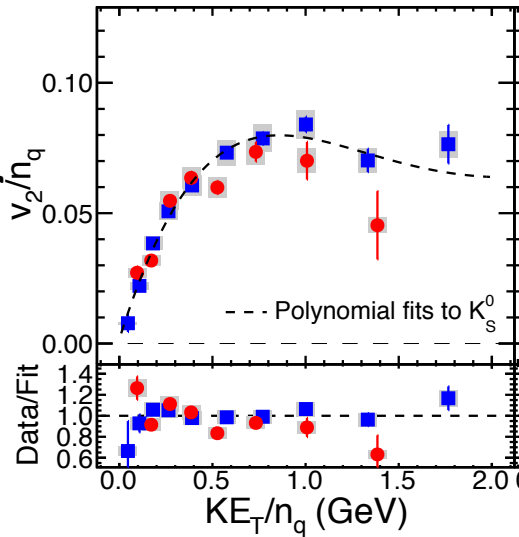
# NCQ scaled $v_2$ in pp collisions compared to pPb and PbPb



CMS PAS HIN-16-010



Phys.Lett.B 742 (2015) 200

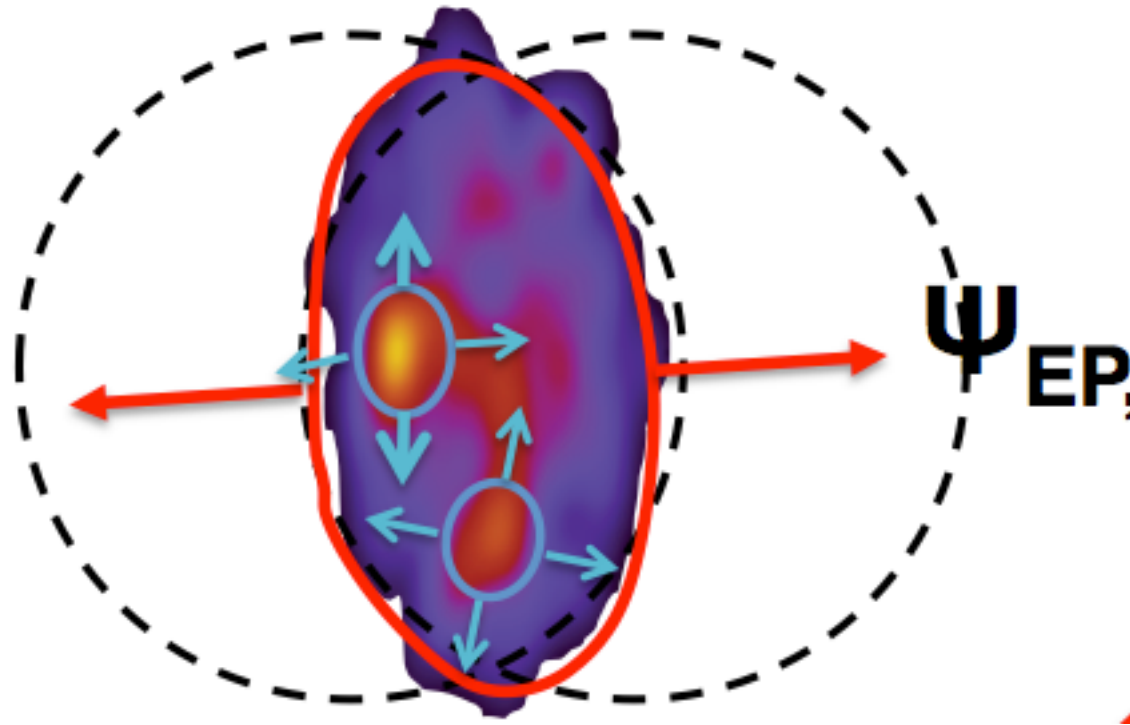


Phys.Lett.B 742 (2015) 200

collectivity!

❖ Significant magnitude of the NCQ scaled  $v_2$  in  $pp$ , comparable to the ones seen in pPb and PbPb collisions

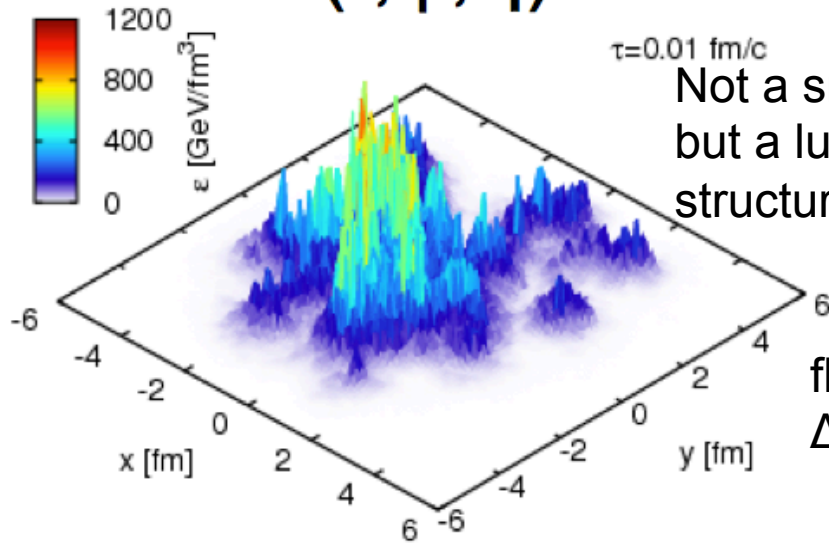
# Factorization breaking – $p_T$ dependent event plane fluctuations



# Initial-state inhomogeneity

Initial state

$$\varepsilon(r, \varphi, \eta)$$

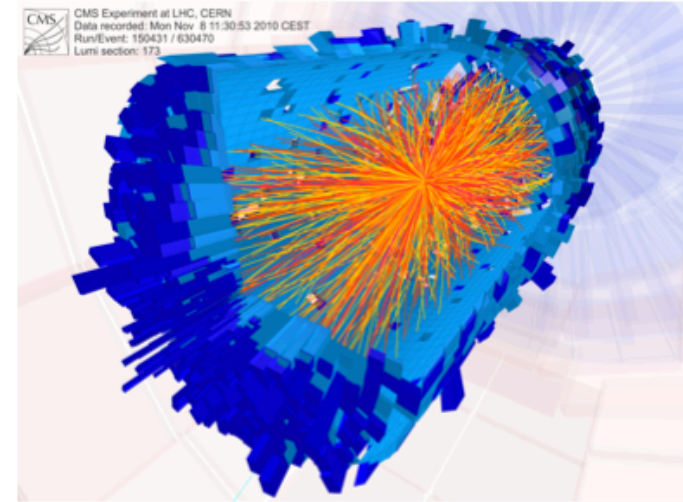


overlap zone in x-y

EbE hydro.

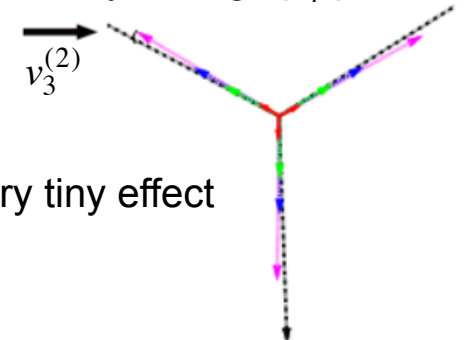
Final state

$$f(p_T, \varphi, \eta)$$



- ✧ The goal is to map initial-state and its fluctuations in 3D
- ✧ Local hotspots perturb the EP of a smooth medium, so  $\Psi_n(p_T)$  contains information about initial-state fluctuations Phys.Rev.C **92** (2015) 034911
- ✧ Within hydrodynamics, initial-state fluctuations could appear as (sub-leading) flows

only for high- $p_T$  particles



Example: sub-leading triangular flow

# Factorization breaking

- ❖ How to connect  $v_n(p_T)$  and  $V_{n\Delta}(p_T)$ ?
- ❖ Usual assumption that EP angle  $\Psi_n$  does not depend on  $p_T$  leads to factorization

$$V_{n\Delta}(p_{T1}, p_{T2}) = \sqrt{V_{n\Delta}(p_{T1}, p_{T1})} \times \sqrt{V_{n\Delta}(p_{T2}, p_{T2})} = v_n(p_{T1}) \times v_n(p_{T2})$$

- ❖ [Gardim et al., PRC 87 \(2013\) 031901](#) and [Heinz et al., PRC 87 \(2013\) 034913](#) proposed that not only  $v_n$  depends on  $p_T$ , but also  $\Psi_n$  could depend on  $p_T$  due to event-by-event (EbE) fluctuating initial state
- ❖ then:

$$V_{n\Delta}(p_{T1}, p_{T2}) = \left\langle v_n(p_{T1}) v_n(p_{T2}) \cos \left[ n(\Psi_n(p_{T1}) - \Psi_n(p_{T2})) \right] \right\rangle$$
$$\neq \sqrt{V_{n\Delta}(p_{T1}, p_{T1})} \times \sqrt{V_{n\Delta}(p_{T2}, p_{T2})}$$

even if hydro flow is the only source of the correlation

**initial state fluctuations**  $\rightarrow \Psi_n(p_T) \rightarrow$  **factorization breaking**

# Factorization breaking

❖ new observable:  $r_n = \frac{V_{n\Delta}(p_T^{trig}, p_T^{assoc})}{\sqrt{V_{n\Delta}(p_T^{trig}, p_T^{trig})} \sqrt{V_{n\Delta}(p_T^{assoc}, p_T^{assoc})}} =$

$$\frac{\langle v_n(p_T^{trig}) v_n(p_T^{assoc}) \cos [n(\Psi_n(p_T^{trig}) - \Psi_n(p_T^{assoc}))] \rangle}{\sqrt{v_n^2(p_T^{trig}) v_n^2(p_T^{assoc})}} = \begin{cases} 1 & \text{fact. holds} \\ <1 & \text{fact. breaks} \\ >1 & \text{non-flow} \end{cases}$$

❖ Large effect is expected and confirmed in ultra central PbPb collisions

**CMS collaboration: Studies of azimuthal dihadron correlations in ultra-central PbPb collisions at  $\sqrt{s_{NN}} = 2.76$  TeV, JHEP 1402 (2014) 088**

❖ As in pPb collisions initial-state fluctuations play a dominant role could we expect a similar (in size) effect?

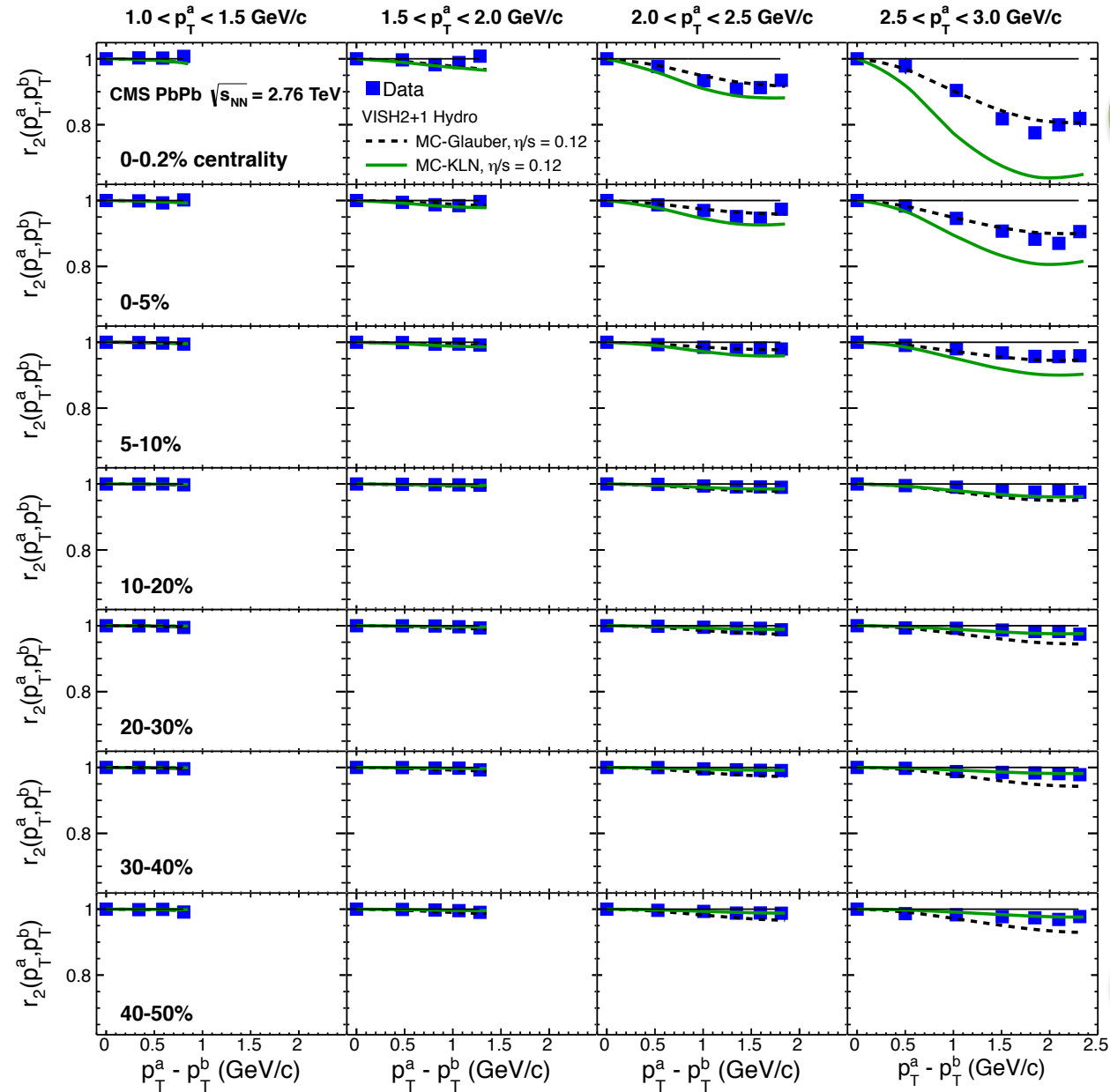
❖ Two hydro models with different initial conditions and  $\eta/s$  were developed:

✧ [Heinz-Shen VISH2+1: PRC 87 \(2013\) 034913](#)

✧ [Kozlov et. al.: arXiv:1405.3976](#)

❖ Constraining of initial conditions and  $\eta/s$  by comparing to the exp. data?

→  $p_T^{trig}$



0-0.2% **PbPb case**



- ❖ The effect increases with rise of  $p_T^{trig}$  and  $p_T^{trig} - p_T^{assoc}$
- ❖ Approaching the central collisions, the effect dramatically increases achieving value over 20%
- ❖ For semi-central collisions, the effect achieves only a size of 2-3%



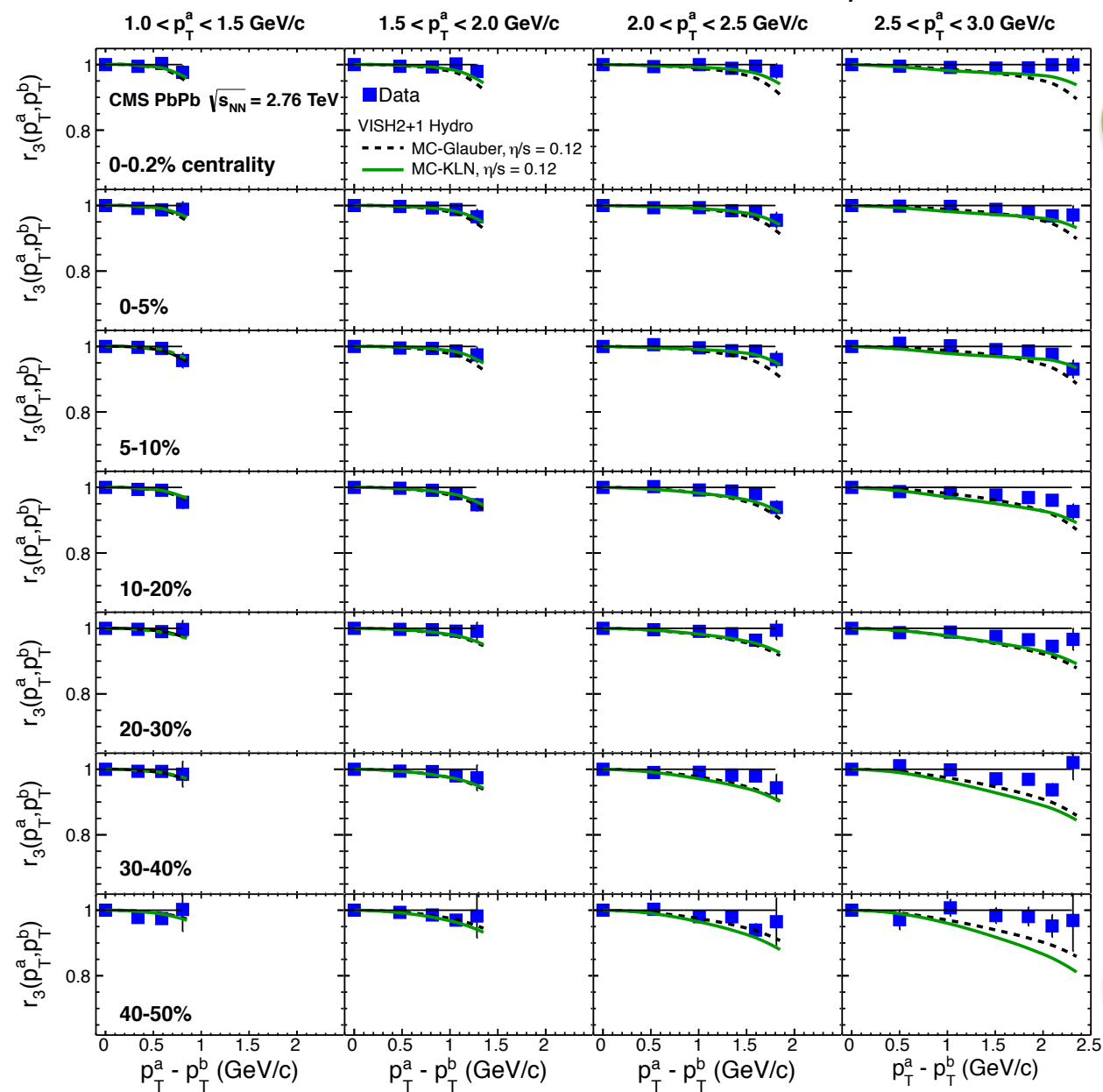
40-50%



**arXiv: 1503.01692**  
**PRC 92 (2015) 034911**



→  $p_T^{trig}$



0-0.2% **PbPb case**

- ❖ Factorization holds better for  $V_3$   
 ❖ Breaking visible only for the highest  $p_T^{trig} - p_T^{assoc}$   
 ❖ Very weakly depends on centrality

40-50%

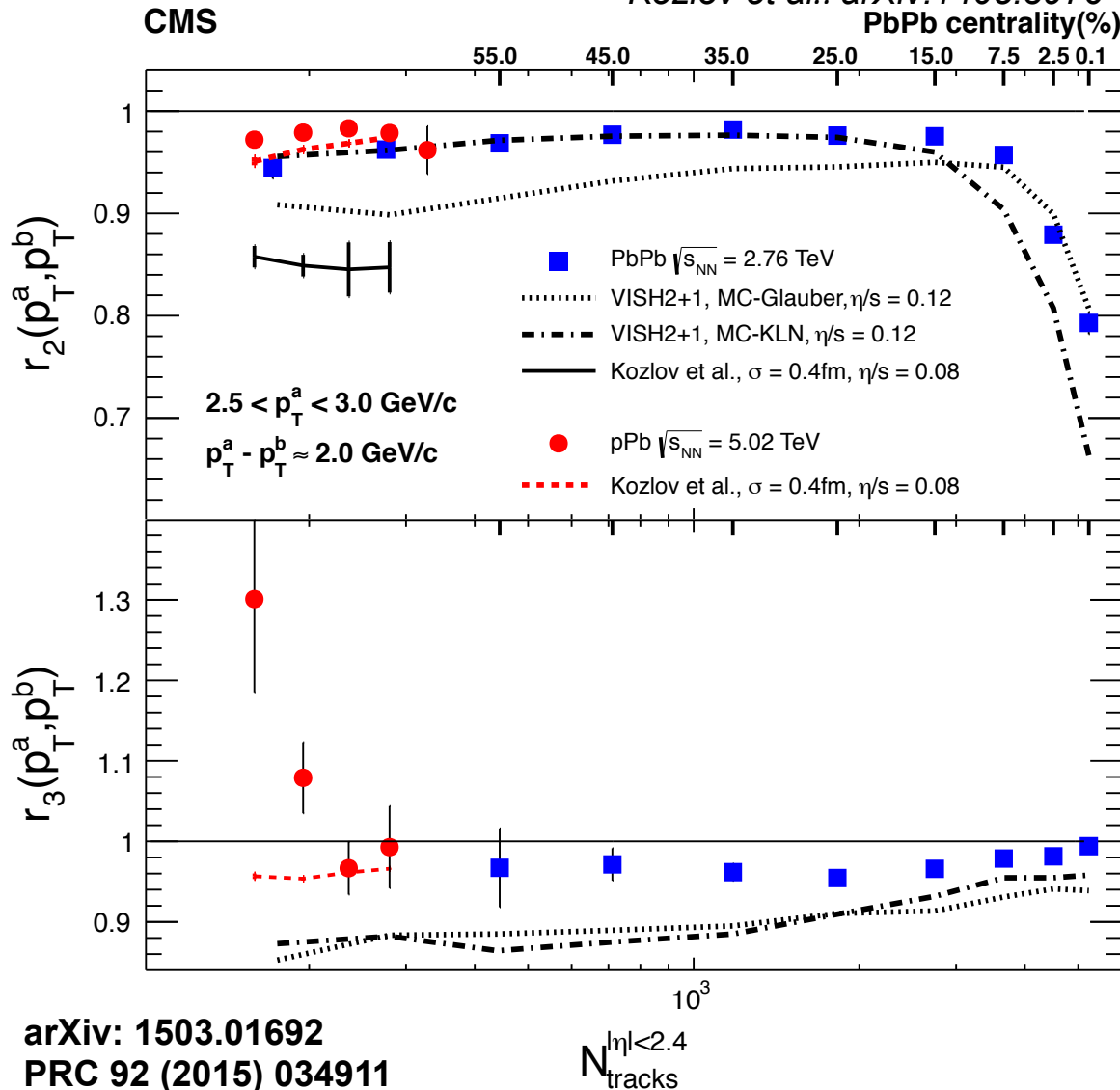
arXiv: 1503.01692  
 PRC 92 (2015) 034911



# $r_n$ multiplicity dependence at the highest $\Delta p_T$

VISH2+1: PRC 87 (2013) 034913

Kozlov et al.: arXiv:1405.3976

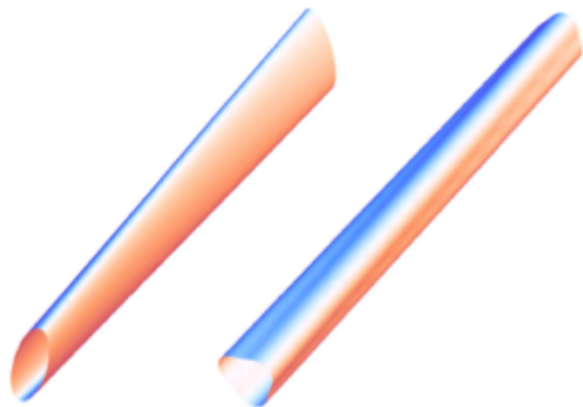


- ◆ Dramatic increase at ultra-central PbPb. For small centralities ( $>5\%$ )  $\approx$  few %
- ◆ The  $r_2$  in pPb is a bit smaller than in PbPb
- ◆ Strong  $r_3$  multiplicity dependence in pPb, but very weak in PbPb
- ◆ A non-flow effect in pPb for the highest  $p_T^{trig}$  in lower multiplicities
- ◆ VISH2+1 qualitatively describes CMS data
- ◆ Kozlov et al. hydro model describes pPb. Gives stronger effect for PbPb and fails for  $r_3$  at lower multiplicity

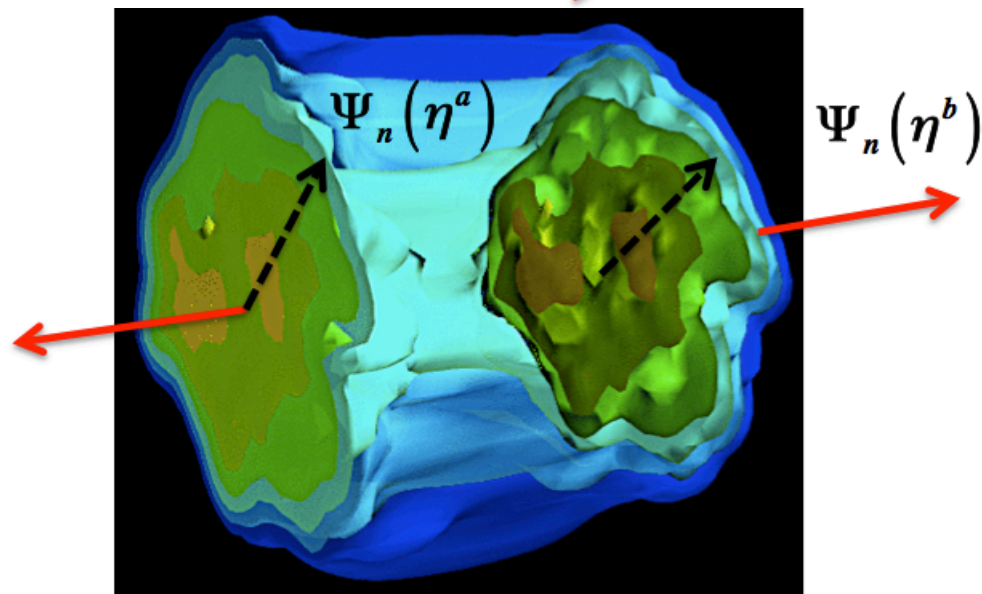
arXiv: 1503.01692  
 PRC 92 (2015) 034911

# Factorization breaking – $\eta$ dependence

$$f(p_T, \phi, \eta) \sim 1 + 2 \sum_{n=1}^{\infty} v_n(p_T, \eta) \cos[n(\phi - \Psi_n(p_T, \eta))]$$



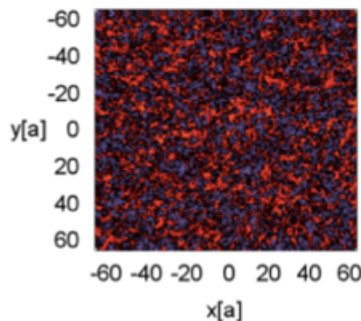
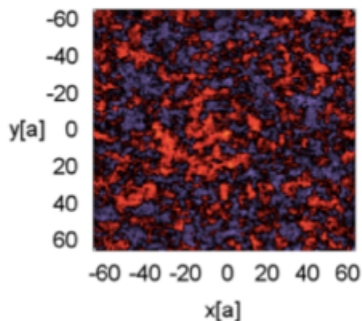
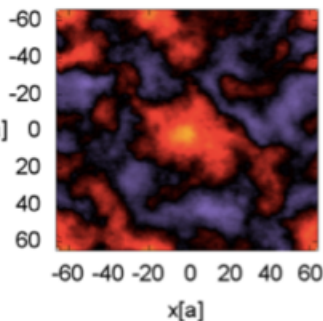
Bozek et al., arXiv: 1011.3354  
Global twist



$Y = 0.0$

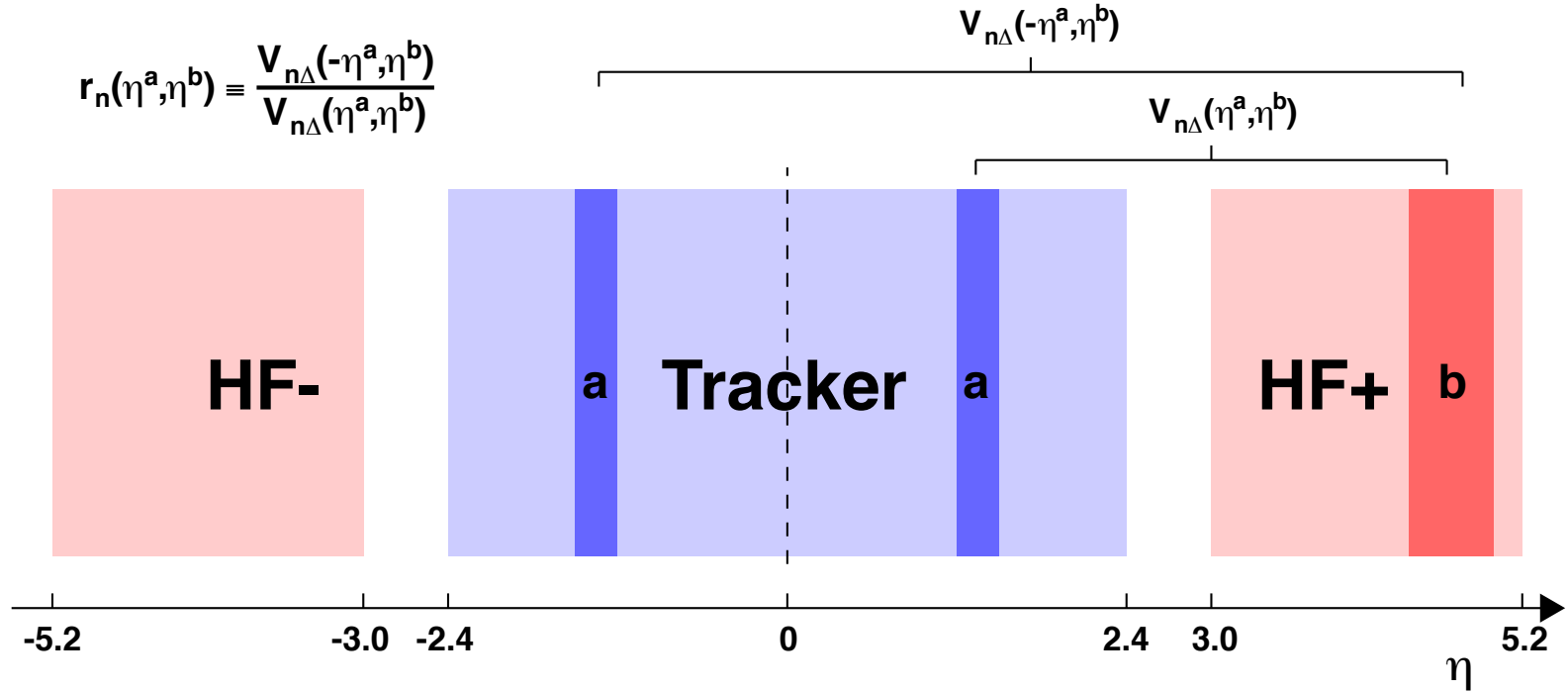
$Y = 5.2$

$Y = 10.4$



Dumitru et al., arXiv: 1108.4764

# $\eta$ -dependent $r_n$ using Hadronic Forward (HF)



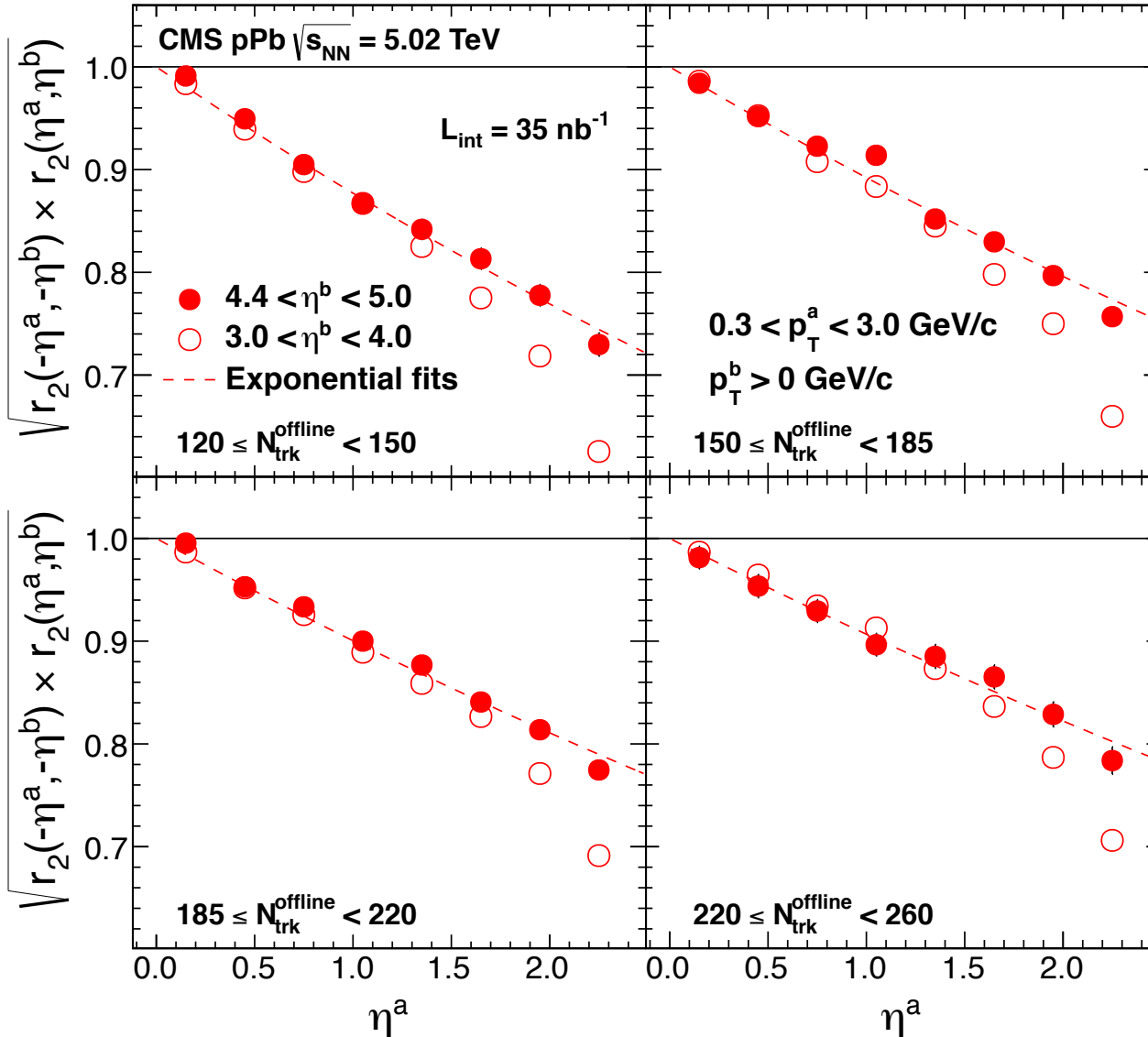
For symmetric collision:

$$r_n(\eta^a, \eta^b) \approx \frac{\langle \cos[n(\Psi_n(-\eta^a) - \Psi_n(\eta^b))] \rangle}{\langle \cos[n(\Psi_n(\eta^a) - \Psi_n(\eta^b))] \rangle}$$

For asymmetric collision:

$$\sqrt{r_n(\eta^a, \eta^b) \times r_n(-\eta^a, -\eta^b)} \approx \sqrt{\frac{\langle \cos[n(\Psi_n(-\eta^a) - \Psi_n(\eta^b))] \rangle \langle \cos[n(\Psi_n(\eta^a) - \Psi_n(-\eta^b))] \rangle}{\langle \cos[n(\Psi_n(\eta^a) - \Psi_n(\eta^b))] \rangle \langle \cos[n(\Psi_n(-\eta^a) - \Psi_n(-\eta^b))] \rangle}}$$

# $\eta$ -dependent $r_n$ in pPb

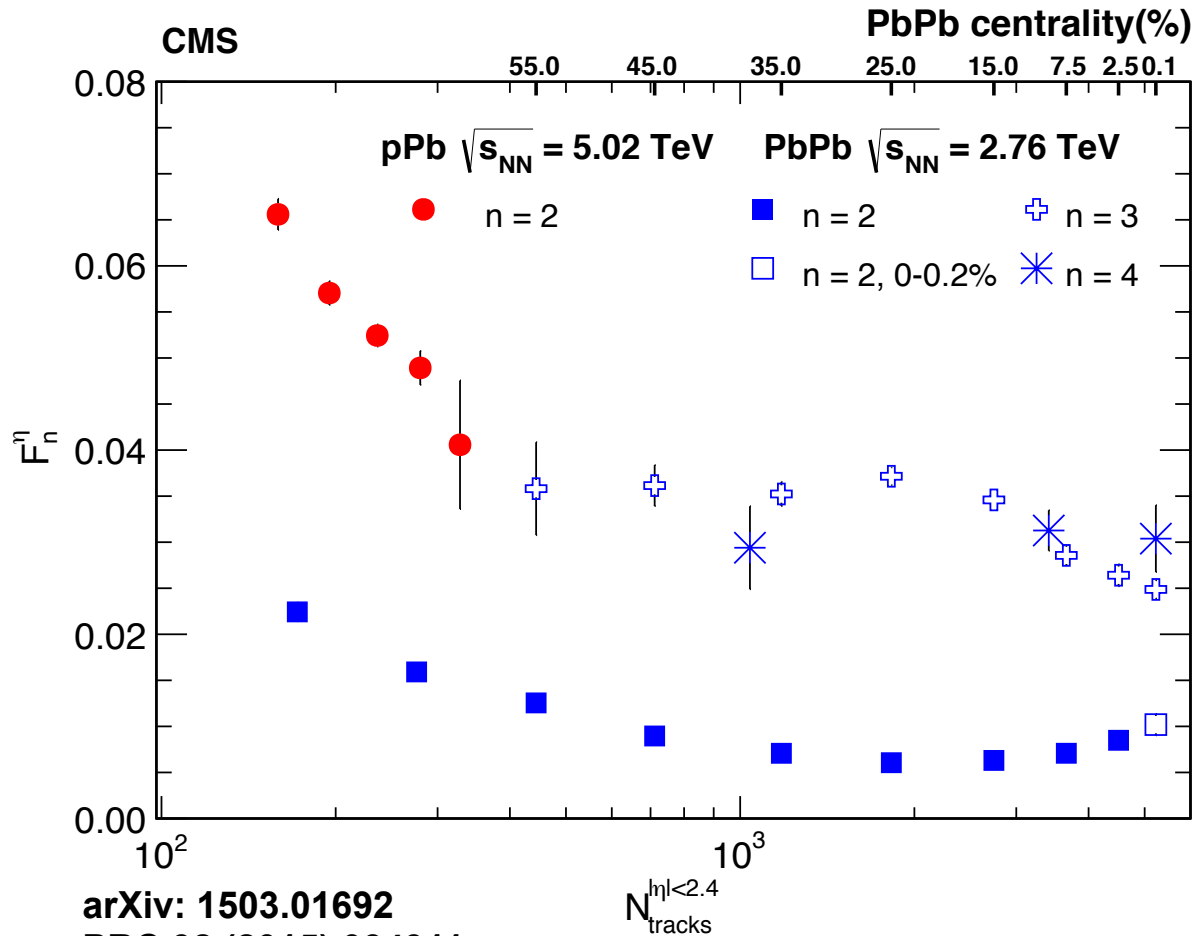


- ❖ A significant factorization breakdown in  $\eta$  found in pPb collisions with increase of  $\eta^a$
- ❖ The effect increases approximately linearly with  $\eta^a$
- ❖ Parameterization with  $F_n^\eta$  is purely empirical introduced just to quantify behavior of the data

$$r_n(\eta^a, \eta^b) \approx e^{-2F_n^\eta \eta^a}$$

arXiv: 1503.01692  
 PRC 92 (2015) 034911

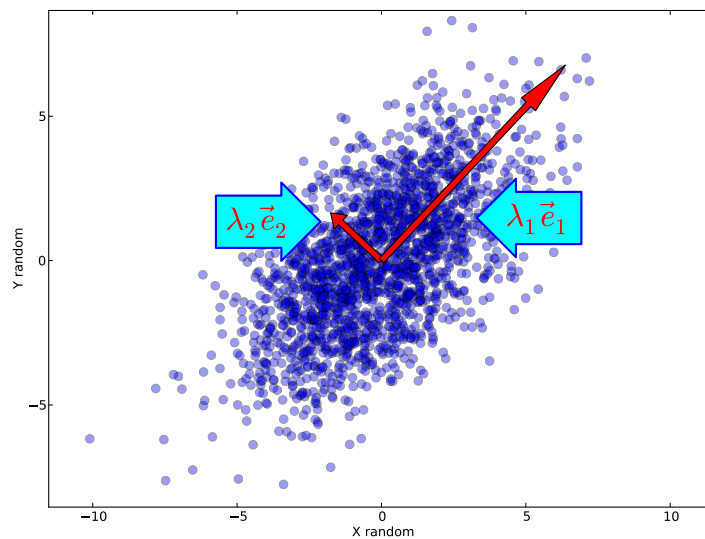
# $\eta$ -dependent $r_n$ vs multiplicity



- ❖ The  $F_2^\eta$  has a minimum around midcentral PbPb and increases for peripheral and most central collisions
- ❖ At similar multiplicity,  $F_2^\eta$  in pPb larger than the one in PbPb
- ❖ Except for the most central PbPb, there is a very weak centrality dependence of  $F_3^\eta$

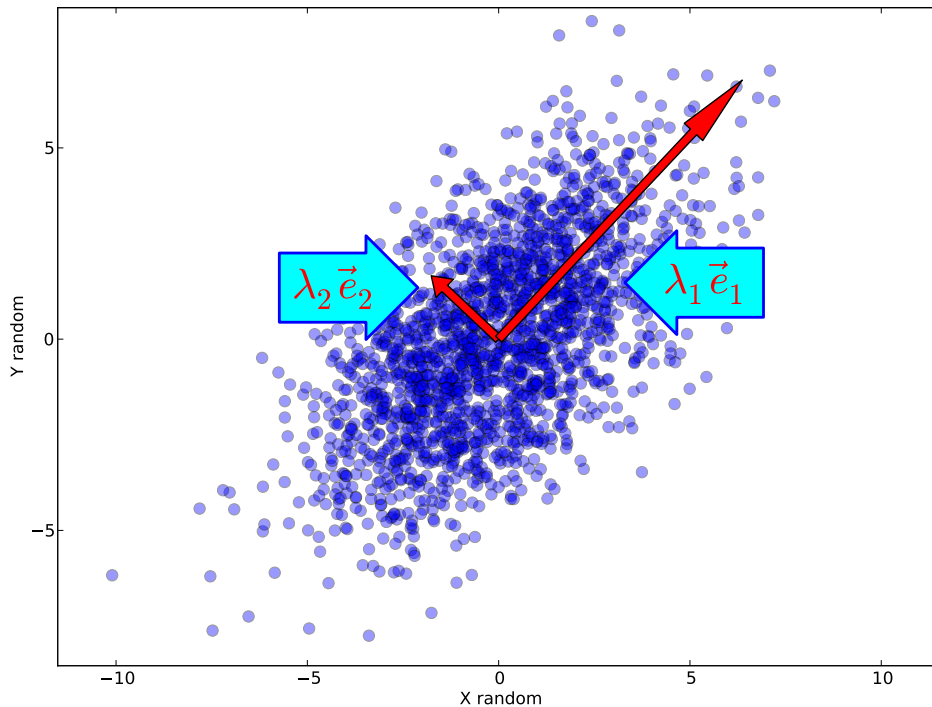
- ❖ In PbPb, higher-orders  $F_3^\eta$  and  $F_4^\eta$ , show much stronger factorization breaking than for the second order

# Principal Component Analysis as a new tool to study flow



# Principal Component Analysis (PCA) method

## A simple 2D example



- ❖ Random data generated by 2D multivariate Gauss distribution

$$\vec{X}_n = (x_1, x_2, \dots, x_n)$$

$$\vec{Y}_n = (y_1, y_2, \dots, y_n)$$

- ❖ a matrix

$$\Sigma = \begin{bmatrix} \text{var}(X) & \text{cov}(X, Y) \\ \text{cov}(X, Y) & \text{var}(Y) \end{bmatrix}$$

- ❖ eigenvectors  $e_i$  and eigenvalues  $\lambda_i$  by diagonalization  $\Sigma$

$$[e]^T \Sigma [e] = \text{diag}(\lambda_1, \lambda_2)$$

- ❖ **First Principal Component:** eigenvector  $e_1$  points to maximum variance of data cloud. Its magnitude is  $\sqrt{\lambda_1} e_1$
- ❖ **Second Principal Component:** eigenvector  $e_2$  points to the next maximum variance of data cloud. Its magnitude is  $\sqrt{\lambda_2} e_2$

# PCA method in hydrodynamic flow - prescription

Two very recent theoretical papers: [R.S.Bhalerao, J-Y. Ollitrault, S.Pal and D.Teaney, Phys.Rev.Lett. 114 \(2015\) 152301](#) and [A.Mazeliauskas and D.Teaney, Phys.Rev. C91 \(2015\) 044902](#) introduced the PCA as a new method to study hydrodynamics flows

- ❖ “The simplest correlations are *pairs*. The **principal component analysis** is a method which extracts *all* the information from pair correlations in a way which facilitates comparison between theory and experiment.” J.-Y. Ollitrault

*In this analysis:*

- ❖ **Input:** two-particle Fourier coefficients measured as

PhysRev.C **92** (2015) 034911

*arXiv:1503.01692*

*and other CMS analyses*

$$V_{n\Delta} = \left\langle \left\langle \cos(n\Delta\phi) \right\rangle \right\rangle_S - \left\langle \left\langle \cos(n\Delta\phi) \right\rangle \right\rangle_B \quad \text{where}$$

$\left\langle \left\langle \cos(n\Delta\phi) \right\rangle \right\rangle_S$  and  $\left\langle \left\langle \cos(n\Delta\phi) \right\rangle \right\rangle_B$  are calculated for pairs with  $|\Delta\eta| > 2$

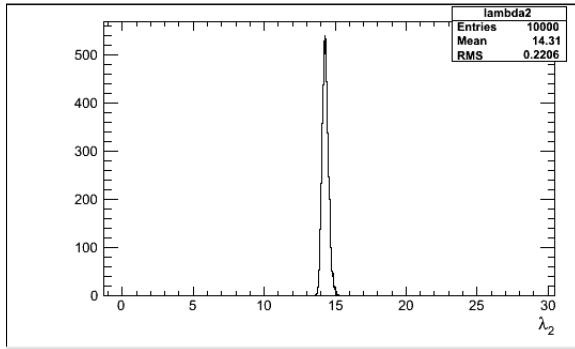
- ❖ 7  $p_T$  bins ( $0.3 < p_T < 3.0$  GeV/c); the eigenvalue problem of a matrix  $[V_{n\Delta}(p_i, p_j)]$

$$\begin{pmatrix} e^{(1)} & e^{(2)} & \dots & \dots & e^{(7)} \end{pmatrix} \begin{bmatrix} V_{n\Delta}(p_1, p_1) & V_{n\Delta}(p_2, p_1) & V_{n\Delta}(p_3, p_1) & \dots & \dots & \dots & \dots \\ V_{n\Delta}(p_1, p_2) & V_{n\Delta}(p_2, p_2) & V_{n\Delta}(p_3, p_2) & \dots & \dots & \dots & \dots \\ V_{n\Delta}(p_1, p_3) & V_{n\Delta}(p_2, p_3) & V_{n\Delta}(p_3, p_3) & \dots & \dots & \dots & \dots \\ \dots & \dots & \dots & \dots & \dots & \dots & \dots \\ \dots & \dots & \dots & \dots & \dots & \dots & \dots \\ \dots & \dots & \dots & \dots & \dots & V_{n\Delta}(p_7, p_7) & \dots \end{bmatrix} \begin{pmatrix} e^{(1)} \\ e^{(2)} \\ \dots \\ \dots \\ \dots \\ \dots \\ e^{(7)} \end{pmatrix} = \text{diag} \left( \lambda^{(1)} \quad \lambda^{(2)} \quad \dots \quad \lambda^{(7)} \right)$$



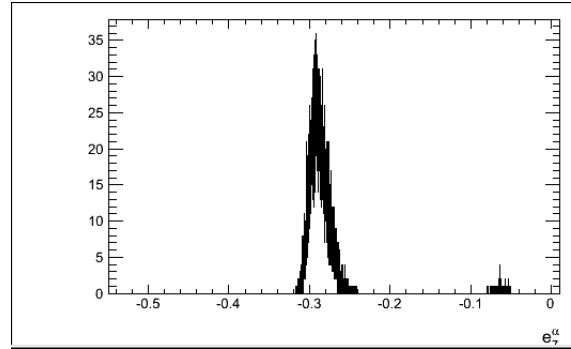
# PCA method in hydrodynamic flow - prescription

$\lambda$  distribution,  $\alpha=2$



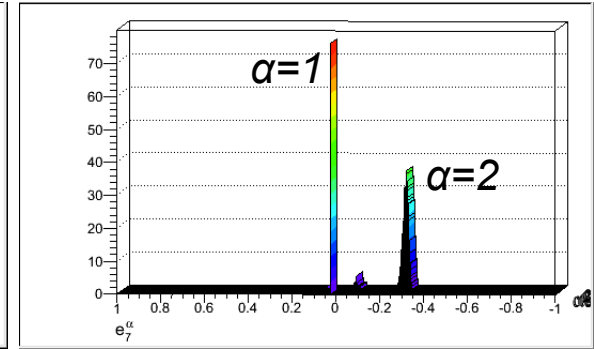
CMS Preliminary

$e$  distribution,  $\alpha=2$



$2.5 < p_T < 3.0 \text{ GeV}/c$

$\alpha=2$  signal 200 times smaller wrt  $\alpha=1$



- ❖ The new introduced  $p_T$  dependent variable, **flow mode**, is defined as

$$V_n^{(\alpha)}(p_i) = \sqrt{\lambda^{(\alpha)}} e^{(\alpha)}(p_i) \quad \text{where } \alpha=1, \dots, 7$$

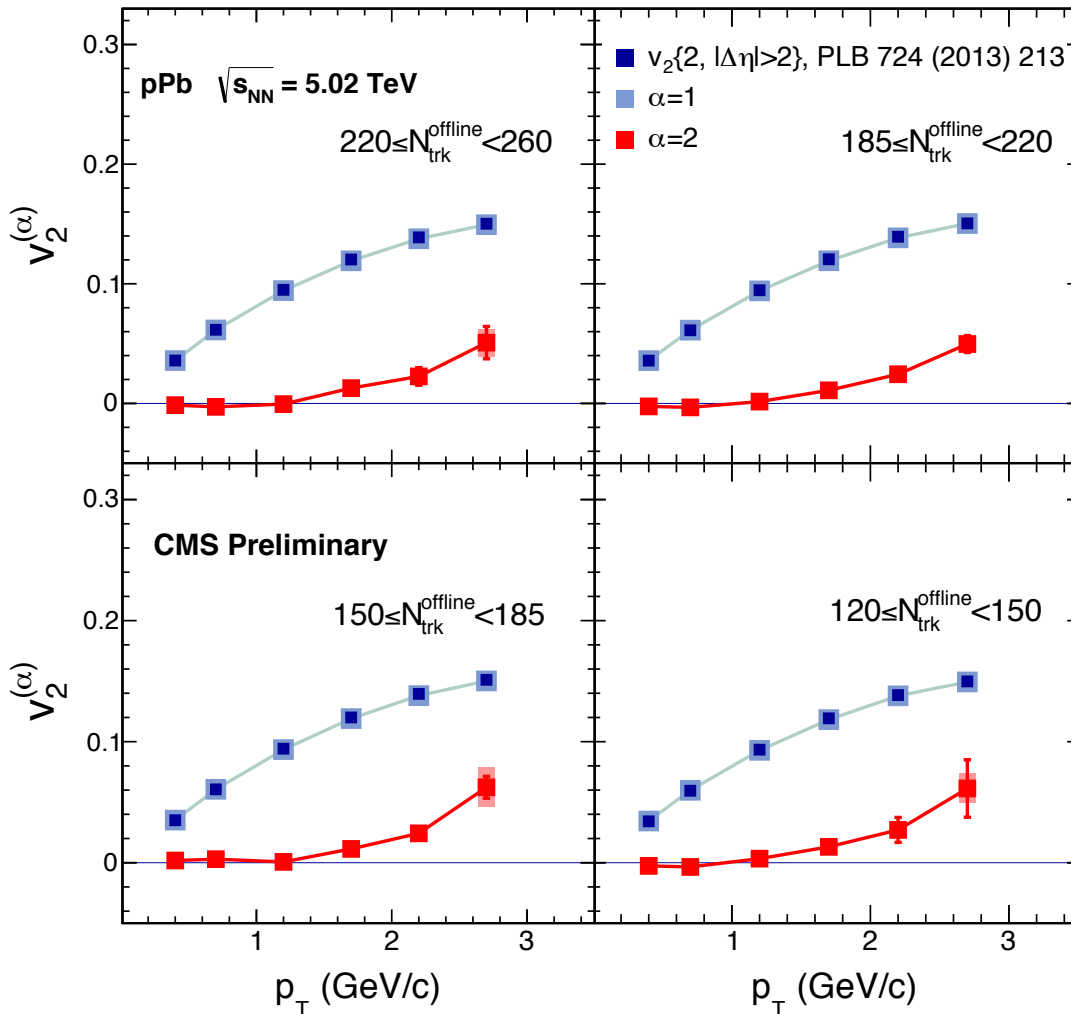
- ❖ corresponding single-particle flow mode  $v_n^{(\alpha)}(p) = \frac{V_n^{(\alpha)}(p)}{\langle M(p) \rangle}$

- ❖ experimental data  $\rightarrow V_{n\Delta}(p_i, p_j) \rightarrow$  it has its own statistical error  $\Delta V_{n\Delta}(p_i, p_j)$

- ❖ The error propagation through  $V_n^{(\alpha)}$  up to  $v_n^{(\alpha)}$

- ❖  $\Delta\lambda^\alpha$  and  $\Delta e^\alpha$  as RMS of the distributions like ones shown above. Matrix elements  $V_{n\Delta}$  were perturbed (10k times) within its  $\Delta V_{n\Delta} \rightarrow$  matrix  $[V_{n\Delta}]$  **nonlinearly** perturbed

# Results – elliptic flows in pPb collisions

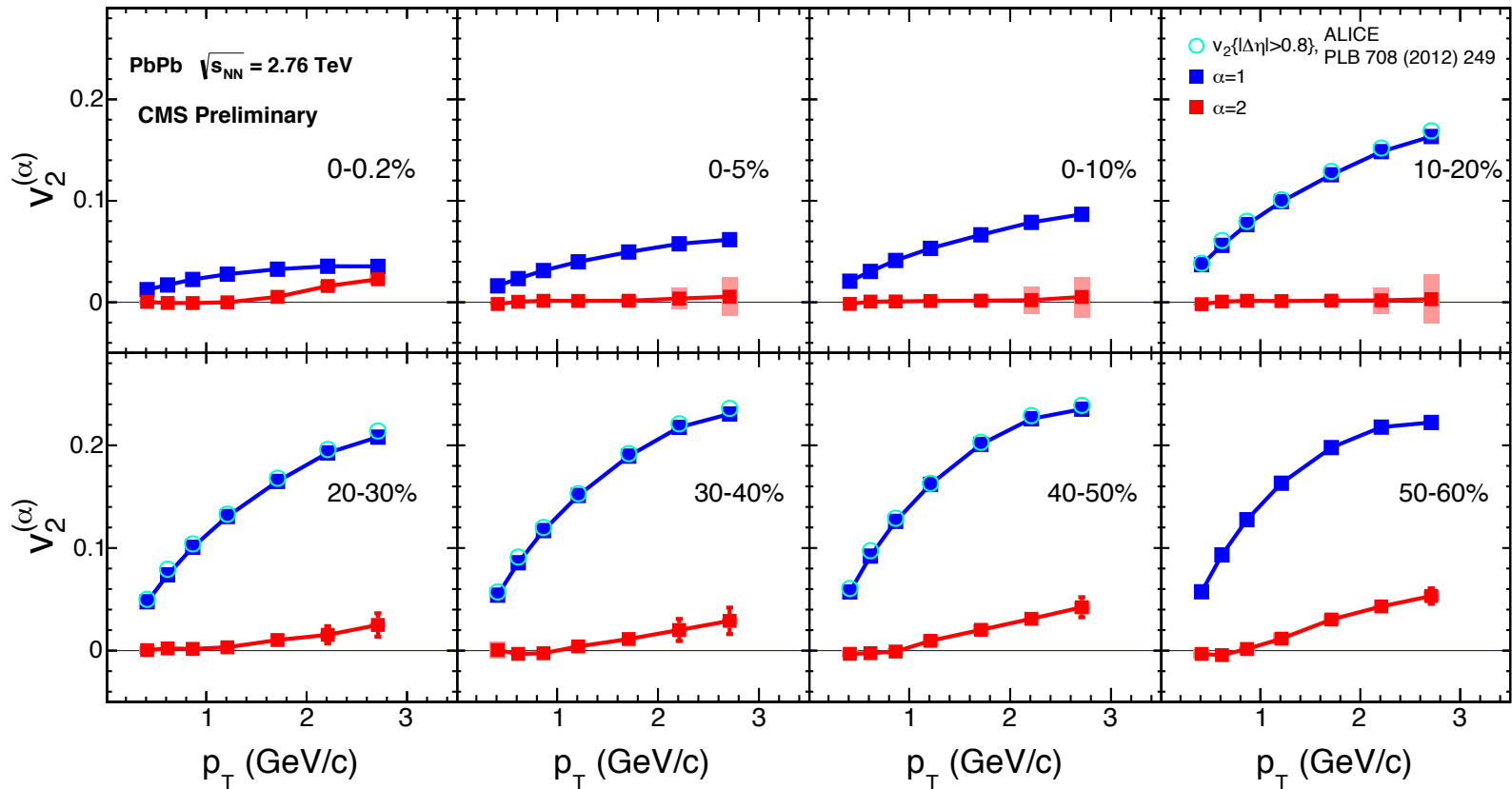


- ❖ The leading flow mode,  $\alpha=1$ , practically identical to the  $v_2$  measured using two-particle correlations
- ❖ The sub-leading flow mode,  $\alpha=2$ , is essentially equal to zero at small  $p_T$  and increases up to 4-5% going to the high- $p_T$

**CMS PAS HIN-15-010**

- ❖ The first experimental measurement of the elliptic sub-leading flow
- ❖ Systematical uncertainties small or comparable to statistical ones only at high- $p_T$

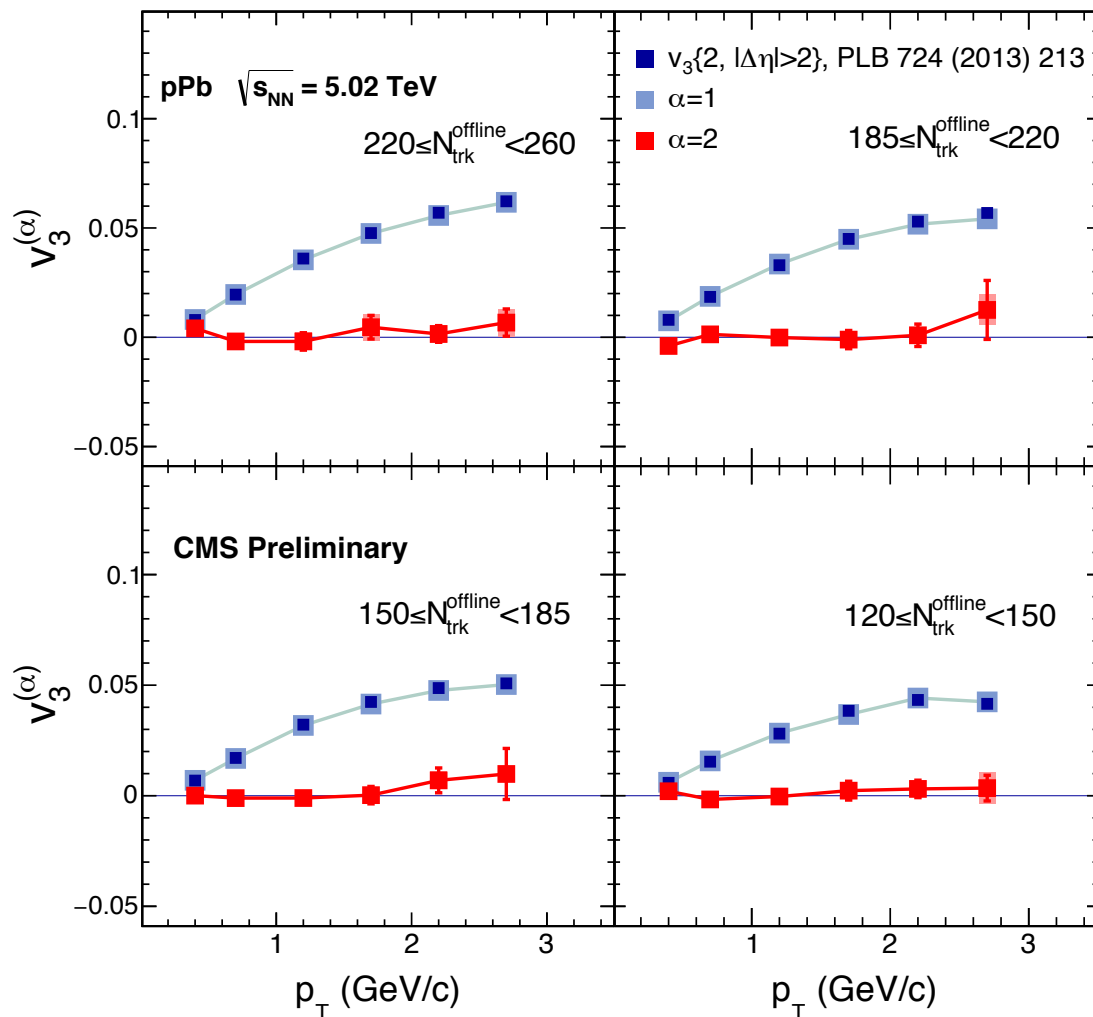
# Results – elliptic flows in PbPb collisions



CMS PAS HIN-15-010

- ❖ The leading flow mode,  $\alpha=1$ , essentially equal to the  $v_2$  measured by ALICE using two-particle correlations
- ❖ The sub-leading flow mode,  $\alpha=2$ , is positive at UCC and for collisions with centralities above 20%
- ❖ In the region 0-20% centrality comparable with zero
- ❖ Similar behavior wrt the  $r_2$  results (10.1103/PhysRevC.92.034911, arXiv: 1503.01692)

# Results – triangular flows in pPb collisions

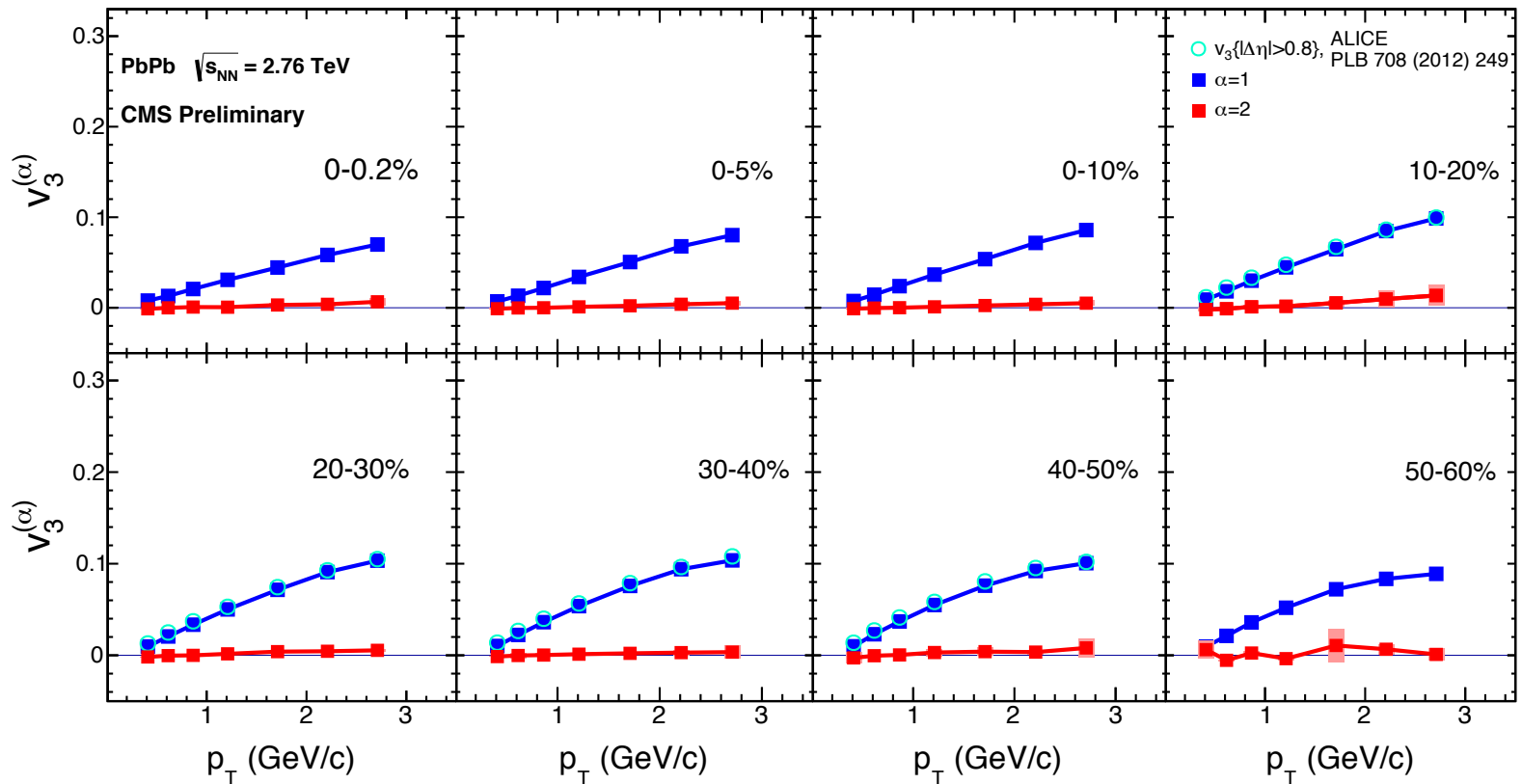


- ❖ The leading triangular flow mode,  $\alpha=1$ , nearly identical to the  $v_3$  measured using two-particle correlations
- ❖ The sub-leading flow mode,  $\alpha=2$ , is comparable with zero within the given uncertainties.

CMS PAS HIN-15-010

- ❖ The first experimental measurement of the triangular sub-leading flow

# Results – triangular flows in PbPb collisions

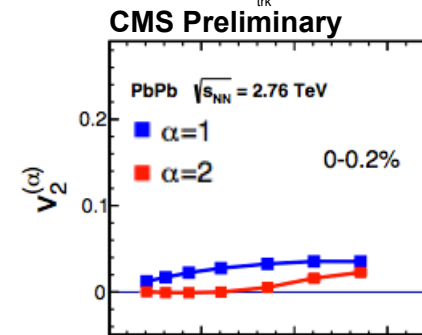
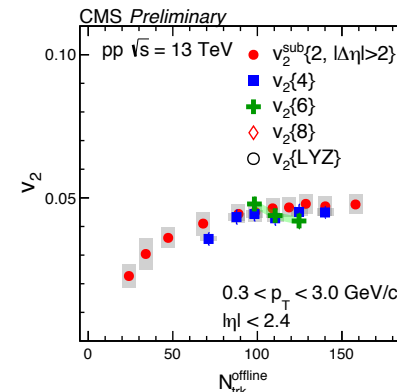
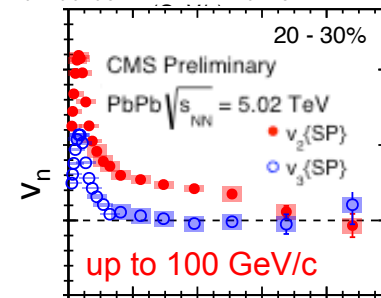
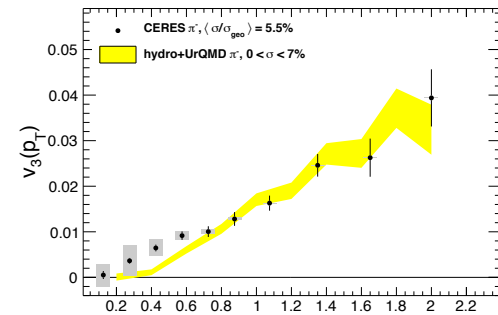


CMS PAS HIN-15-010

- ❖ Again, the leading flow mode,  $\alpha=1$ , essentially equal to the  $v_3$  measured by ALICE using two-particle correlations
- ❖ The sub-leading flow mode,  $\alpha=2$ , is, within the uncertainties, equal to zero
- ❖ Results have a similar centrality dependence to that observed for  $r_3$  (Phys. Rev C **92** (2015) 034911, *arXiv: 1503.01692*)

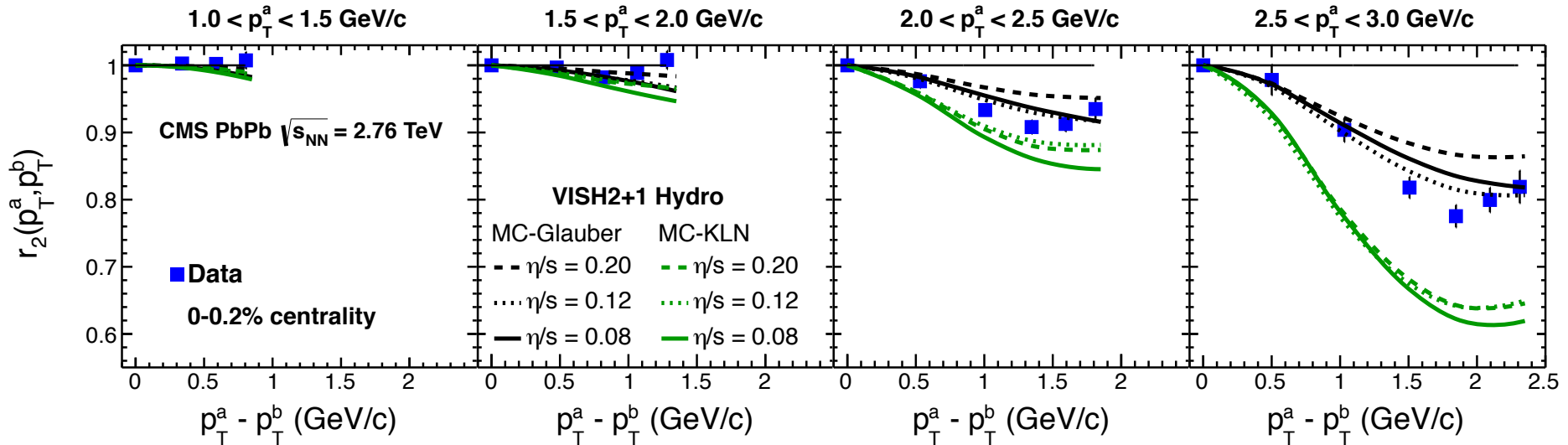
# Conclusions

- ❖ The first  $v_3(p_T)$  measurement at the top SPS energy with CERES using the event plane method
- ❖ The  $v_2$  and  $v_3$  measured up to 100 GeV/c in PbPb at 5 TeV
- ❖ The  $v_2$  and  $v_3$  in small pPb and smallest pp system formed in collisions at the LHC energies
- ❖ A strong factorization breaking effect for  $n=2$  appears approaching UCC PbPb collisions
- ❖ The sub-leading flow modes are for the first time experimentally measured in both pPb and PbPb collisions at the LHC energies
- ❖ The sub-leading elliptic flow modes is in a qualitative agreement with the  $r_2$  factorization-breaking results
- ❖ The sub-leading triangular flow modes in both collision system is small if not zero showing that the triangular flow factorizes much better than the elliptic flow
- ❖ These results could help in better understanding of the initial-state fluctuations



# Backup slides

# $r_2$ in ultra-central PbPb collisions and VISH2+1



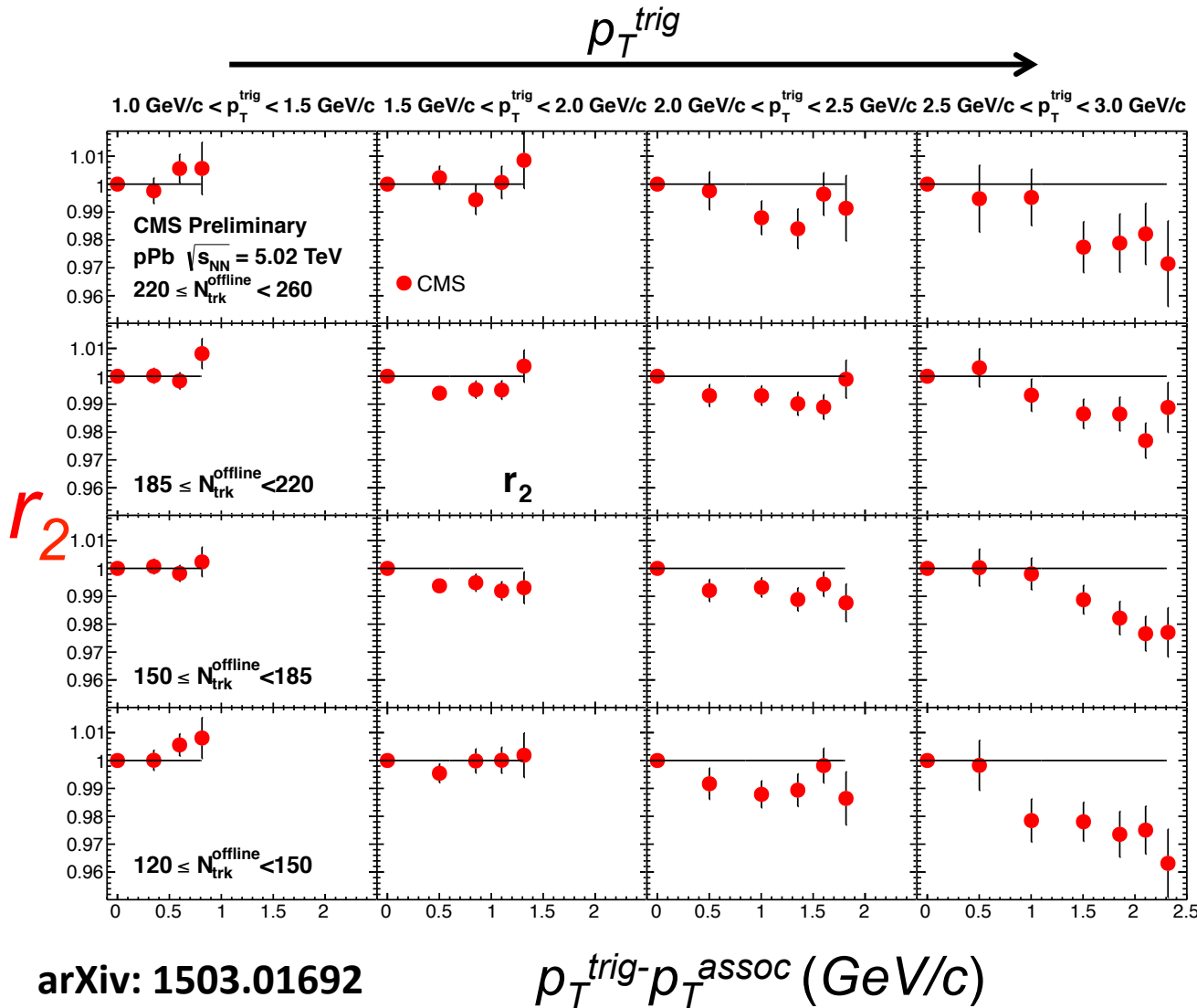
arXiv: 1503.01692, PRC 92 (2015) 034911

VISH2+1: PRC 87 (2013) 034913

- ❖ The effect increases with rise of  $p_T^{trig}$  and  $p_T^{trig} - p_T^{assoc}$
- ❖ The biggest effect seen in ultra-central collisions while for semi-central collisions, the effect achieves only a size of 2–3%
- ❖ The VISH2+1 model qualitatively gives a good description of CMS data for both MC-Glauber and MC-KLN initial conditions
- ❖ Large insensitivity to  $\eta/s$  → an independent constraint to the initial-state



# $r_2$ from high-multiplicity pPb collisions



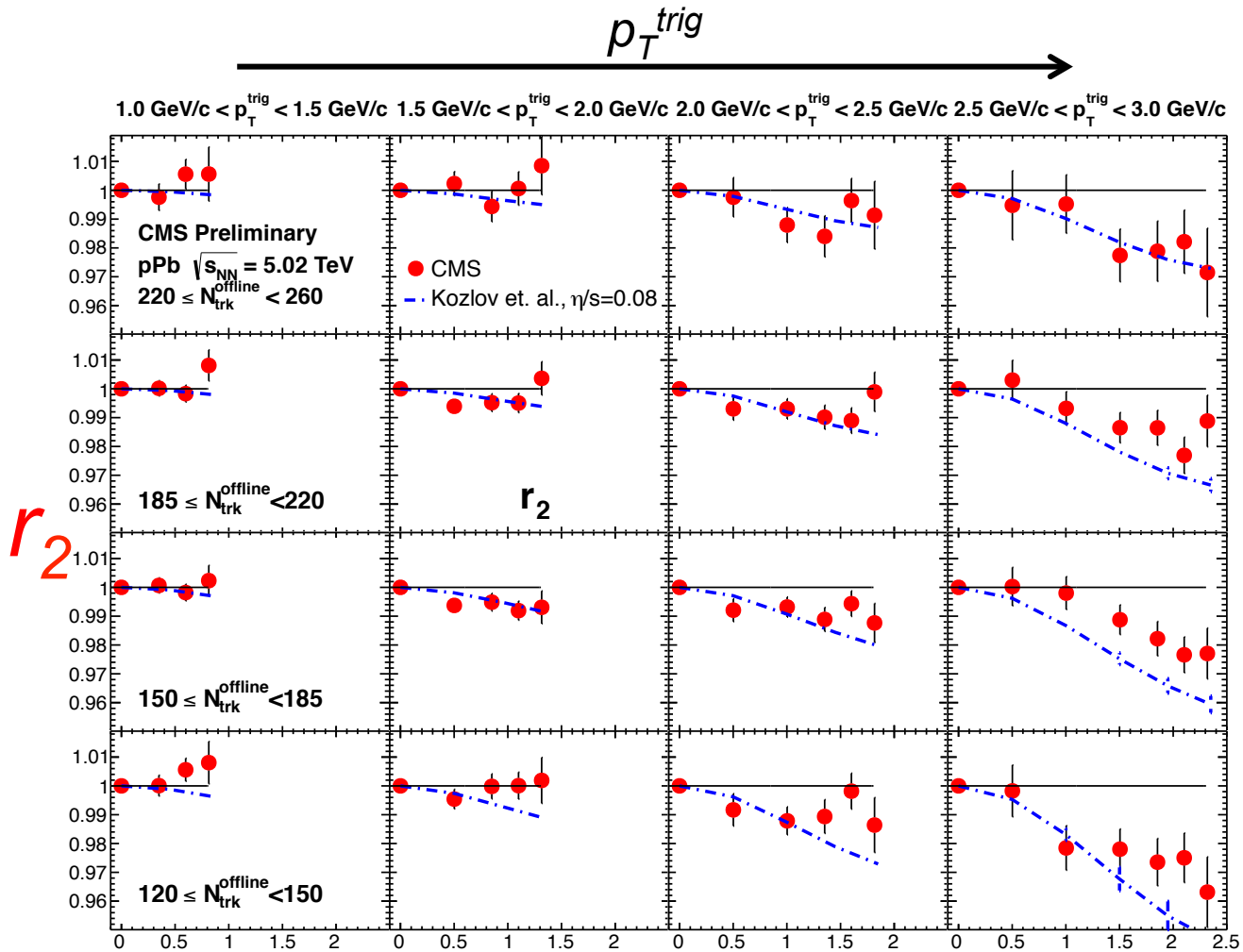
$220 < N_{trk}^{offline} < 260$

- ◆ The effect increases with  $p_T^{trig}$  and  $p_T^{trig} - p_T^{assoc}$
- ◆ Maximum around 2-3%
- ◆ Nearly no dependence on multiplicity

$120 < N_{trk}^{offline} < 150$

arXiv: 1503.01692  
PRC 92 (2015) 034911

# pPb $r_2$ : comparison to Kozlov et. al hydro model



$220 < N_{trk}^{offline} < 260$

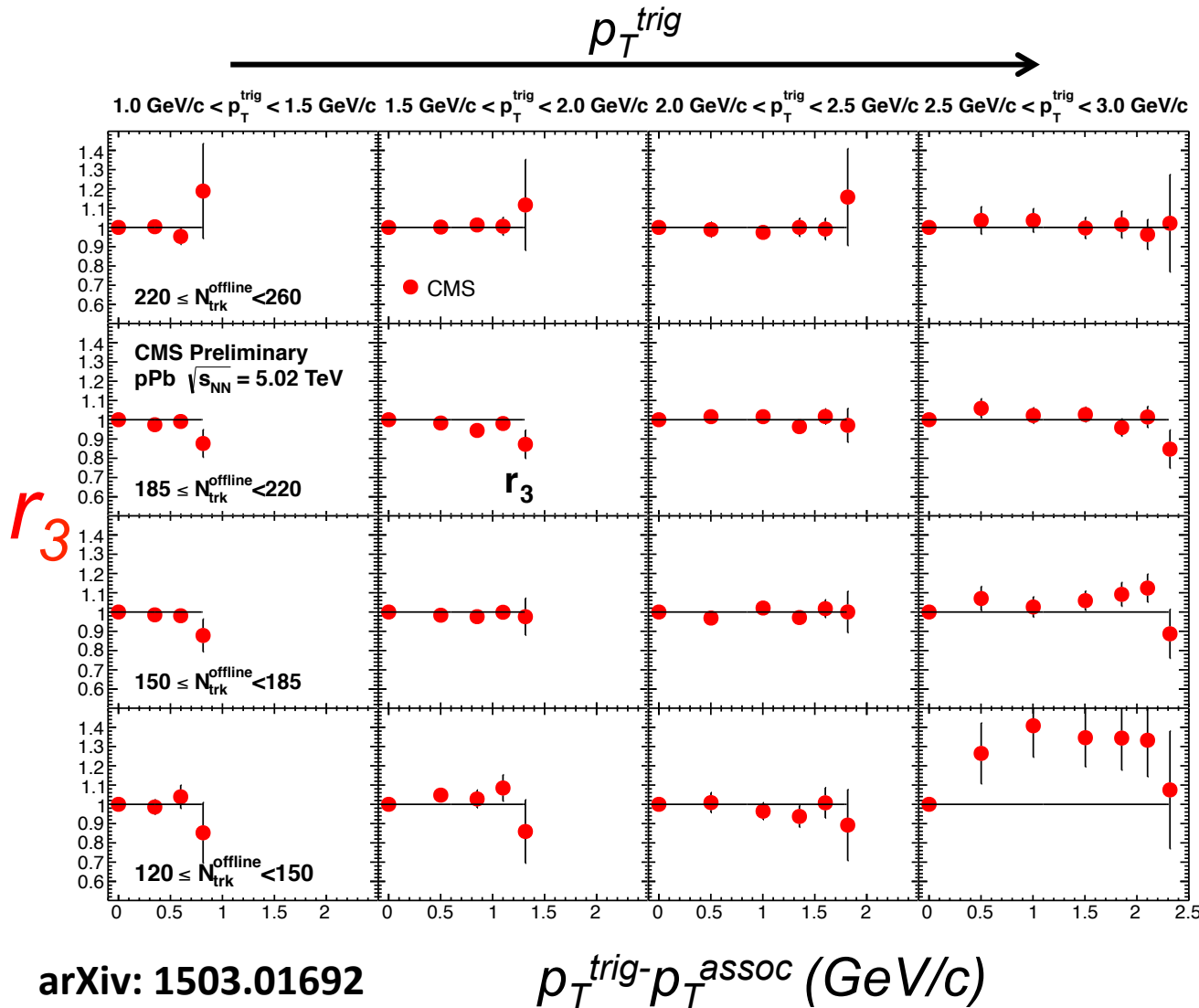
Kozlov et al. hydro model qualitatively describes data

$120 < N_{trk}^{offline} < 150$

arXiv: 1503.01692  
 PRC 92 (2015) 034911

$p_T^{trig} - p_T^{assoc}$  (GeV/c)   Kozlov et al.: arXiv:1405.3976

# $r_3$ from high-multiplicity pPb collisions



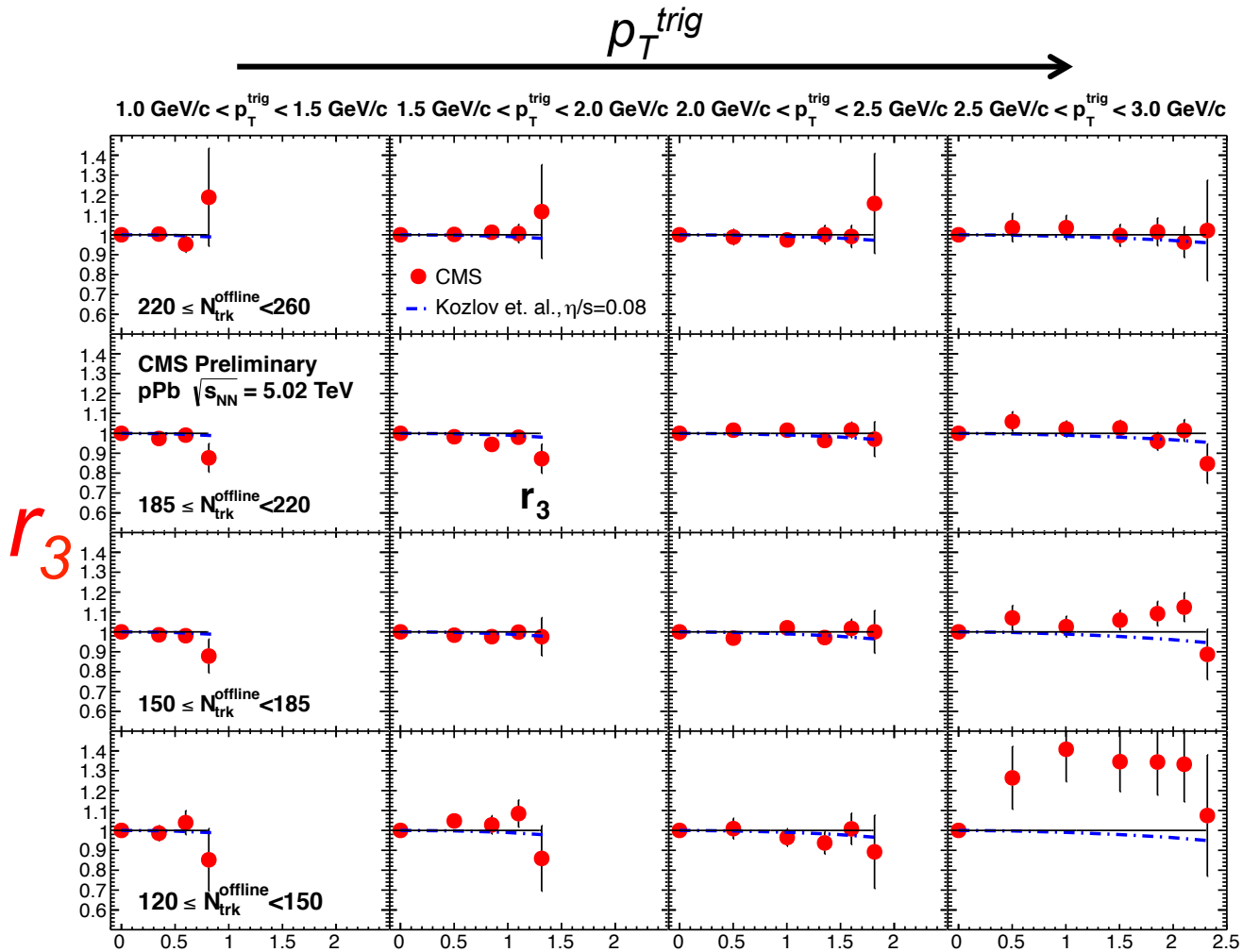
$220 < N_{trk}^{offline} < 260$

- ❖  $V_3$  factorize better than  $V_2$
- ❖ A direct indication of non-flow effect seen in  $r_3$  for the highest  $p_T^{trig}$  in lower multiplicity bins

$120 < N_{trk}^{offline} < 150$

arXiv: 1503.01692  
PRC 92 (2015) 034911

# pPb $r_3$ : comparison to Kozlov et. al hydro model



$220 < N_{trk}^{offline} < 260$

❖ Kozlov et al. hydro model qualitatively describes data except in lower multiplicity bins for the highest  $p_T^{trig}$



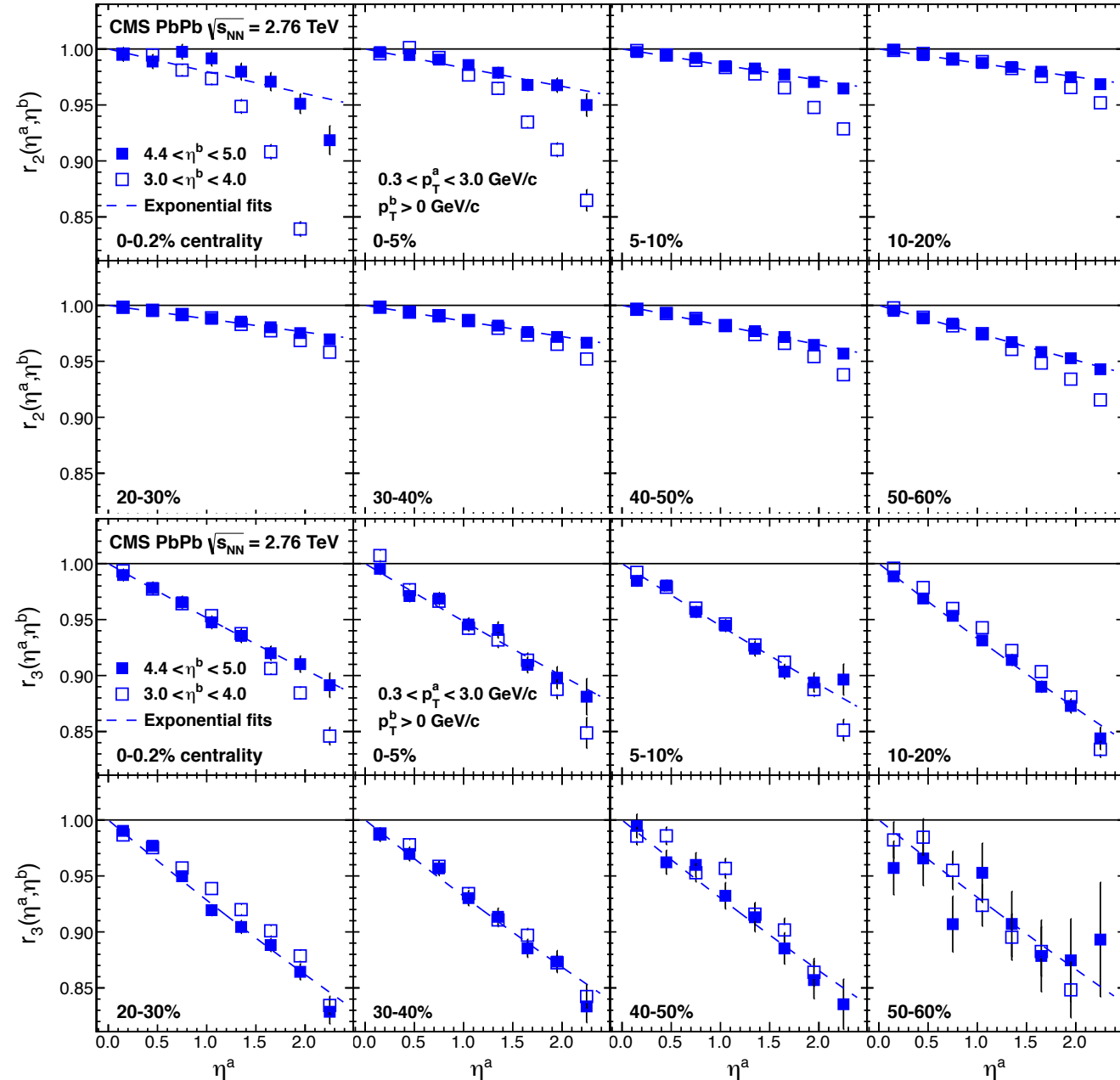
$p_T^{trig}$

$120 < N_{trk}^{offline} < 150$

arXiv: 1503.01692  
PRC 92 (2015) 034911

$p_T^{trig} - p_T^{assoc}$  (GeV/c) Kozlov et al.: arXiv:1405.3976

# $\eta$ -dependent $r_n$ in PbPb



- ❖ The  $r_2$  factorization breaking effect increases with increase of  $\eta^a$
- ❖ Except for the most central collisions, the increase is approximately linear

arXiv: 1503.01692  
 PRC 92 (2015) 034911

- ❖ The effect of factorization breaking is much stronger for higher-order harmonic  $r_3$  – opposite to the  $p_T$  dependence
- ❖ Almost linear increase of the effect size
- ❖ Parameterization:

$$r_n(\eta^a, \eta^b) \approx e^{-2F_n^\eta \eta^a}$$

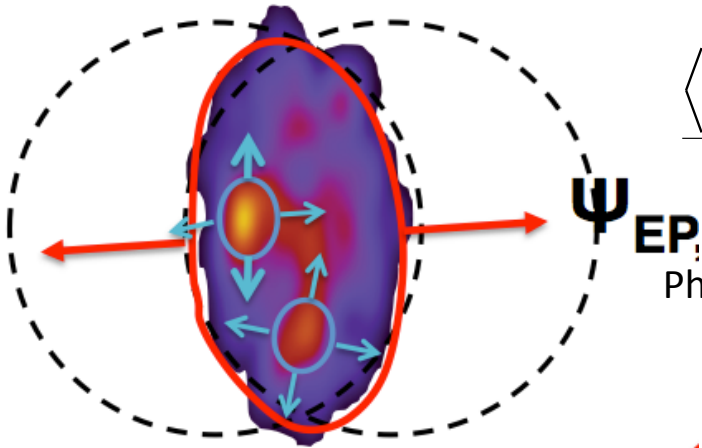
# Factorization breaking - connection to the PCA

- ❖ Initial-state fluctuations  $\rightarrow$  the EP ( $\Psi_n$ ) depends on  $p_T$  and on  $\eta \rightarrow$  factorization is broken. New observable

introduced:

$$r_n = \frac{V_{n\Delta}(p_{T1}, p_{T2})}{\sqrt{V_{n\Delta}(p_{T1}, p_{T1})} \sqrt{V_{n\Delta}(p_{T2}, p_{T2})}} =$$

$$\frac{\langle v_n(p_{T1}) v_n(p_{T2}) \cos[n(\Psi_n(p_{T1}) - \Psi_n(p_{T2}))] \rangle}{\sqrt{v_n^2(p_{T1})} \sqrt{v_n^2(p_{T2})}} = \begin{cases} 1 & \text{holds} \\ < 1 & \text{brakes} \\ > 1 & \text{non-flow} \end{cases}$$

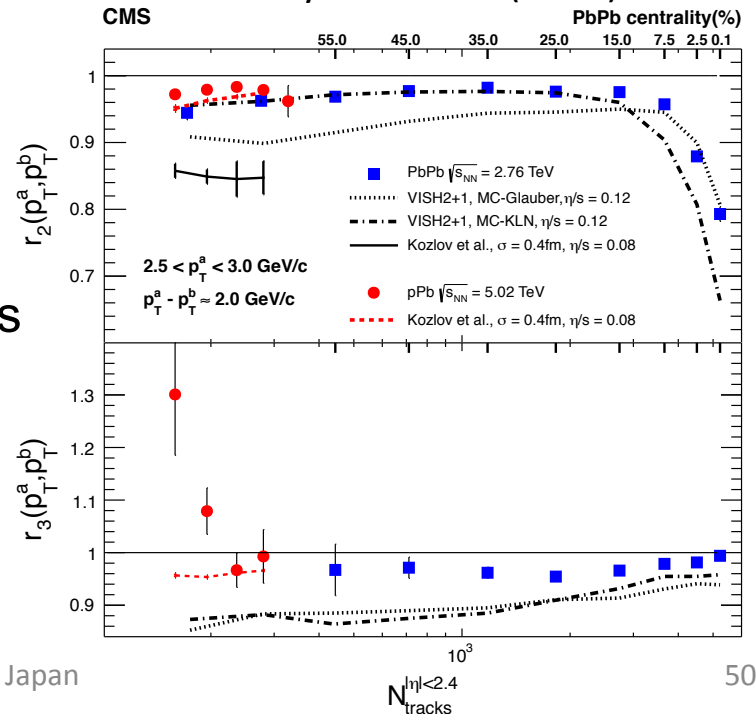


Phys.Rev. C87 (2013) 031901

Phys.Rev. C87 (2013) 034913

- ❖ If there is only one principal component for each harmonic  $n \rightarrow V_{n\Delta}(p_i, p_j)$  factorizes

- ❖  $r_n$  i.e.  $V_{n\Delta}(p_i, p_j)$  results are partially integrated, while mutually orthogonal eigenmodes contain all information



Phys. Rev. C 92 (2015) 034911  
(arXiv:1503.01692)

# Factorization breaking - connection to the PCA

- ❖ The given harmonic order  $n$  has also higher ( $\alpha > 2$ ) eigenmodes ordered from largest to smallest, while in  $r_n$  they are not clearly distinguished
- ❖ The PCA can approximately reconstruct two-particle  $V_{n\Delta}(p_i, p_j)$  coefficients

$$V_{n\Delta}(p_i, p_j) \approx \sum_{\alpha=1}^{k \leq N_b} V_n^{(\alpha)*}(p_i) V_n^{(\alpha)*}(p_j) \quad \text{where } N_b = 7$$

which can be used to calculate the factorization breaking ratio  $r_n$

- ❖ So, the PCA is a good tool for analysis in hydrodynamics with fluctuations in the initial state
- ❖ Note that the PCA uses the whole  $p_T$  range simultaneously to extract the information on both leading and sub-leading flow modes

